ASSESSMENT PM10 CONCENTRATION DURING MOVEMENT CONTROL ORDER (MCO) USING REMOTE SENSING DATA AND GIS TECHNIQUE IN JOHOR BAHRU

NURSYAHREEN AQILAH BINTI MOHMAD RASSID
2016709445

CENTRE OF STUDIES FOR SURVEYING SCIENCE AND GEOMATICS
FACULTY OF ARCHITECTURE, PLANNING AND SURVEYING
UNIVERSITI TEKNOLOGI MARA MALAYSIA

FEBRUARY 2021

ASSESSMENT PM10 CONCENTRATION MONITORING DURING MOVEMENT CONTROL ORDER (MCO) USING REMOTE SENSING DATA AND GIS TECHNIQUE IN JOHOR BAHRU

NURSYAHREEN AQILAH BINTI MOHMAD RASSID

2016709445

Thesis submitted to the Universiti Teknologi MARA Malaysia
in partial fulfilment for the award of the degree of the
Bachelor of Surveying Science and Geomatics (Honours)

FEBRUARY 2021

DECLARATION

I declare that the work on this project/dissertation was carried out in accordance with the regulations of Universiti Teknologi MARA (UiTM). This project/dissertation is original and it is the result of my work, unless otherwise indicated or acknowledged as referenced work.

In the event that my project/dissertation be found to violate the conditions mentioned above, I voluntarily waive the right of conferment of my degree of the Bachelor of Surveying Science and Geomatics (Honours) and agree be subjected to the disciplinary rules and regulations of Universiti Teknologi MARA.

Name of Student	:	Nursyahreen Aqilah Binti Mohmad Rassid
Student's ID No	:	2016709445
Project/Dissertation Title	:	Assessment PM10 Concentration during Movement Control Order (MCO) using Remote Sensing and GIS Technique in Johor Bahru
Signature and Date	:	

Approved by:

I certify that I have examined the student's work and found that they are in accordance with the rules and regulations of the Department and University and fulfils the requirements for the award of the degree of Bachelor of Surveying Science and Geomatics (Honours)

Name of Supervisor	:	Prof. Madya Sr. Dr. Siti Aekbal Binti Salleh
Signature and Date	:	

ABSTRACT

The COVID-19 pandemic and associated lockout lowered pollution levels in major megacities around the world, including Malaysia. The Malaysia Movement Control Order (MCO) was then introduced in 2020 with the goal of isolating the origins of the outbreak of COVID-19. The aim of the study is to monitor the elements of parameters such as particulate matter (PM_{10}) using medium spatial resolution remote sensing imagery for distinguish changes the amount of particles using Landsat 8 Operational Land Imager (OLI) satellite data around study area. The Air Pollutant Index (API) data acquired by the Department of Environment Malaysia on an hourly basis before and during the MCO with the goal of monitoring changes in fine particulate matter (PM10) on a separate algorithm model. The findings demonstrate that the proposed multispectral PM_{10} model can estimate concentrations of particulate matter with a reasonable degree of precision. The study proved the efficiency of their multispectrum estimation model with PM10 concentration based on Landsat 8 OLI band which can be seen in satellite images with Johor region. The shows that only a certain algorithm model is measuring the accuracy of concentration of PM10 such as models 3,4,5, and 7. The average spread of PM10 concentration on 10 March 2020 before MCO and 26 March 2020 after MCO was in the range 25 - 136 μg / m3. As a result of the observation, the actual reading of the highest reduction was in model 5 with 47.14% (Before = 48.85 μg / m 3; During MOC = 25.82 μg / m 3), while the lowest decrease was in model 4, with 19.20% (decrease at 23.03 μg / m 3). This shows a pattern of air quality decreased by 47.14% and a decrease in value between before and after MCO with -23.03 μg / m 3. As a result, less motor cars were on the road and the operation of the sector was halted, thus minimizing the emissions of toxic pollution contaminants in the atmosphere.

ACKNOWLEDGEMENT

Assalamualaikum wbt,

First of all, I would like to thank my supervisor Asoc. Sr. Dr. Siti Aekbal Binti Salleh for her patience and guidance thus supporting in helping me during the completion of this study. We are very grateful with their willingness to share their knowledge and experience with us. Besides my supervisor, I would like to thank my coordinator Sr. Dr. Abdul Rauf Abdul Rasam and Dr. Nabilah Naharudin for their guidance and support in helping for the completing my thesis paper. Special thanks also to my lovely parents for their unstoppable support and encouragement for me through the completion of this study. Last but not least, thanks to all my fellow friends Anis Anhar, Enis Shazira, Faten Najwa, Nur Nabilah Idzni, Rabiah Anwar, Baggio anak John, Leonney Lioho and all my dearest classmate from AP2208A for the helpful discussions, sleepless night when we were working together from home during this pandemic season of COVID-19 to complete all submissions before the deadlines.

TABLE OF CONTENTS

LIST OF FIGURES

LIST OF TABLES

LIST OF ABBREVIATIONS

COVID-19	Coronavirus Disease 2019
MCO	Movement Control Order
CO	Carbon Monoxide
SO_2	Sulfur Dioxide
NO_2	Nitrogen Dioxide
O_3	Ozone
PM_{10}	Particular Matter
API	Air Pollutant Index
GIS	Geographic Information Systems
DOE	Department of Environment
EPA	Environmental Protection Agency
WHO	World Health Organization
RMG	Recommended Air Quality Guidelines
IPU	Input Pencemaran Udara
APIMS	Air Pollutant Index of Malaysia
PSI	Pollution Standard Index
USEPA	United States Environmental Protection Agency
CAQM	Continuous Air Quality Monitoring
ASMA	Alam Sekitar Sdn.Bhd
USGS	United States Geological Survey
OIL	Operational Land Imager
TOA	Top of Atmosphere

CHAPTER 1

INTRODUCTION

1.1 Background

The introduction of pollution is a waste product in the natural environment which causes negative impacts. Pollution is the release of chemical compounds or electricity, like noise, heat or light. Contamination, whether indoor or outdoor, implies air pollution. When any harmful smoke, gasses or dust enters the atmosphere, it can cause an incredibly bizarre living environment for humans, plants and animals (Chooi & Yong, 2016). According to (Tiwari et al., 2012), due to rapid urbanization, industrial growth, population growth and fossil fuel combustion, the quality of air in developing nations had already reduced and has had harmful effects on the climate. Nevertheless, the rise in air emissions is most closely related to industrial practices, including large-scale combustion plants that burn aviation fuel or chemicals, biomass burning and commercial vehicles. Developments in the manufacturing sector accelerated in 1980 from 38% to 44% in 2002.

Nature of air pollution and pollution sources, weather conditions, as well as properties of the land surface, has been realized that are affected along with the scope and severity of urban air pollution. Air pressure, wind direction, temperature and speed are the factors that are influenced by the natural factors. Hazy is the atmospheric phenomenon wherein smoke, dust and several dry particles disrupt the visibility of the atmosphere. If exposed for long period, it will cause serious health damage to humans because haze contains dust and smoke particulate matter that is a very small particulate matter. If the relative humidity is less than 80 per cent and the air polluted with dry particles such as PM2.5 and PM10 and gasses such as ozone, nitric oxide, nitrogen dioxide and sulfur dioxide, haze could happen (Hanafi et al., 2018)

In April 1983, the first haze brought considerable disruption to daily life in Malaysia since then, Malaysia always related to haze. The burning of 8 million hectares of land

has caused the spreading of haze and thick clouds of smoke producing approximately 30% of annual global average greenhouse gas. According to (Chee Khoon, 2008), the worst haze pollution in Malaysia history was in Kuching when it has exceeded 850. The occurrence of haze has severely impacted the daily livelihood of the people in and surrounding the countries including the schools in Malaysia were ordered to close, besides the direct effects on human health such as suffering breathing difficulties and vomiting. In 2010, according to data gathered, the number of daily patient visits rose by 31% in the hazy period in Kuala Lumpur. For example, one of the countries affected by haze in Malaysia as a result of forest fires in Indonesia is Johor. According to (Abdul Hamid et al., 2018), during the Southwest Monsoon in 2011 and 2013, air quality condition in Larkin and Pasir Gudang has been classified as unsafe and harmful when a specific matter was registered at 54.12 $\mu g/m^2$ and 56.83 $\mu g/m^2$ in the dry season.

Besides, Malaysia were shocked by the news recently about coronavirus disease 2019 (COVID-19), when COVID-19 was first identified on 25 January on travelers from Hubei, China (Wikipedia, 2020a). Due to the drastic increase in cases, Malaysia Prime Minister announced an action known as the Movement Control order (MCO) which results the closing down of transportation, and travel in and out of Malaysia. This also restricted and decreased local business travel, closed universities, colleges and schools in an attempt to minimize the spread of disease and created a number of quarantines. Enforcement of the first stage of the Movement Control Order (MCO) not only helped to break the COVID-19 chain, has in fact reduce environment pollution as well were followed a reduction of activities such as open burning, vehicle, exhaust emission, industrial stack emission and also the reduction in nitrogen dioxide NO2 pollution was first apparent near Wuhan, China, but eventually spread across the country.

Next, measuring the results of major concentrations of air pollutants including particulate matter (PM_{10}), is defined as Air Pollutant Index (API). In Malaysia, the natural mortality has been found to be significantly associated with a daily mean of Ozone (O3), carbon monoxide (CO), Nitrogen Oxides (NO2) and PM10, (Nur H. Hanafi et al., 2019) which are responsible for heart diseases, chronic lung diseases and acute, also cause the aggravation of existing lung diseases such as asthma and

bronchitis (Shaheen et al., 2017). However, due to the different air pollutant measurements between air monitored in Johor, Pasir Gudang where PM2.5 reading was a huge difference of value to Johor's air quality index AQI measurement in 2018. This then caused confusion among Malaysians as if there is a problem in our API measurement because, during the haze period, PM will be a critical parameter were in this study our only focus on the measurement for PM_{10}.

The general definition used for a number of atmospheric solid particles and liquid droplets is Particulate Matter (PM) which is a significant air pollutant in urban areas. Particularly the concentration and composition of particulate matter from the atmospheric pollution are of interest mainly because of their effect on human health. Building, mining, smelting, and manufacturing are examples of industrial activities where particles can be made of hundreds of different chemicals which some are emitted directly and also it comes in many sizes and shapes. There are two types of the particular matter were particular matter with an aerodynamic diameter of 10 μg/m3 which is smaller than the width of cotton fiber is of concern for environmental problems hence the aerosols with aerodynamic diameters smaller than 2.5 μg are responsible for health hazards (Tiwari et al., 2012).

Generally, for major ecological studies such as air quality assessment, remote sensing technique has been in practice. Proof of remote sensing that may have led to a loss of the heating hole is indeed a major increase in the standard of the air in the area. To carry out air pollution studies, Landsat 8 OIL has been used to exhibit the relation between air pollution monitored data and satellite data by a number of researchers. In the detection and monitoring of several meteorological and environment phenomena the techniques of Remote Sensing have assumed an important role by providing a better understanding of the behaviour associated with their responses climate and biophysical parameters of earth's surface variable, including the temperature of the surface (Shaheen et al., 2017).

Besides that, a computer system that analyses and displays geographically referenced information on the earth's surface is called a geographic information system (GIS). Maps offered analysis benefits to provide a tool with the unique visualization and geographic for GIS technology that manages statistical and spatial data. In agricultural

research and natural management, GIS and modelling are becoming powerful tools (Samanta et al., 2011).

Therefore, this study aimed to measure particulate matter PM_{10} on the air quality monitoring based on atmospheric reflectance values of the visible bands by satellite image in the study area using Landsat 8 (OIL). Mapped temporal both particulate matter concentrations by Landsat 8 data and air pollutant monitored station. Thus, it is to determine the impact of COVID-19 on the pattern of air quality data on March 2020.

1.2 Problem Statement

Malaysia's air pollution in Johor Bahru in 2019 was linked to a rise in the incidence of respiratory disease, which is one of the 10 leading causes of death. Industrial development, motor vehicles, and transfer boundary haze are highly sources of pollutant in this region. The source of pollutants on effect the residents living in an ad within the area are currently due to most of the high impact factories are situated in Pasir Gudang. In other words, rapid development around industrial estates should have increased in the construction of new houses and commercial centers closer to the possible source of contamination.

In 2020, Considering the need for lockdown measures, most countries, including Malaysia, have implemented 'Movement Control Orders' (MCOs) as a prevention step to reduce the deadly spread of this disease. The COVID-19 has led to a decrease in air quality all around the world. Nevertheless, the data on the effects of MCOs on air quality at local scales are still sparse.

The second problem is the impact of COVID-19 to sustainable transportation. Before disease, the rapid development around the industrial area increased with the construction of new homes and commercial centers, thus the use of motor vehicles that were closer to sources of pollution. However, Lockdown's execution has resulted in factories and roads shutting, reducing emission. Significant changes in air quality pattern can be identified compared to before, during, and after situations.

The changes of air pollutant due to COVID-19 are almost inaccessible and give a difficulty in producing a map and communicating the details of distribution of impact COVID-19 to the public efficiently. But with technology like GIS, which displays layers of complex data on the maps, it has developed to track how the reduction in released particle emission affects the concentration of air pollution. It also is able to see the levels of air pollution in a given region, and how they differ from nearby areas. In that case, the Image satellite based remote sensing can help in study and solution methods allow various physical features to be monitored simultaneously over vast areas, with an observational density proportionate to the sensor's spatial resolution.

Although, the ambient air quality in Pasir Gudang where, unfortunately, there is the lack of study and assessment to measure the air pollutants concentration by air monitored stations and using satellite imagery to display their distribution. Thus, due to the COVID-19 pandemic has not only brought about a new normal in the lives of the society but has also breathed new life into the environment.

1.3 Aim

The aim of the study is to monitor such as particulate matter (PM_{10}) using medium spatial resolution remote sensing imagery to distinguish changes in amount of particles around the study area. In order to fulfill the objective, the following is set out:

i. To measure the Particulate Matter (PM_{10})
ii. To determine the impacts of MCO to the pattern of air quality
iii. To map the distribution of air pollutant for research area

1.4 General Methodology

In order to fulfill the objective and desired results of the analysis, a systematic approach as shown in Figure 1.1 is created. Overall, this methodology of this study are divided into five levels are following;

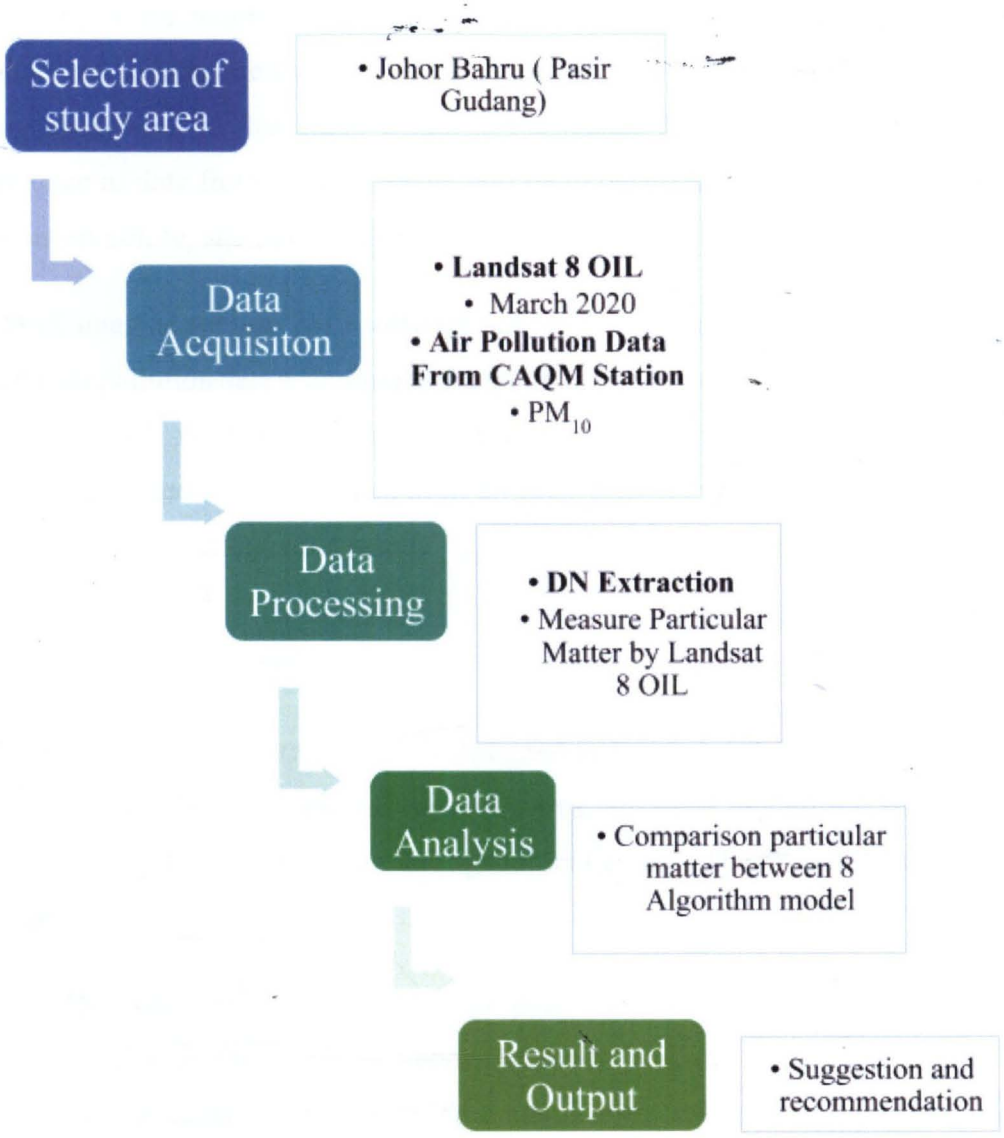

Figure 1.1 Flowchart of methodology

1.5 Scope and Limitation of Study

The research is basically based on the data collected from three air monitored station of Pasir Gudang in the south of Johor over a period of one year in 2018 with selected three dates in the same year which is 6 March 2020 and 26 March 2020.

Johor has about a measure air monitoring stations across the city that are currently identified as the number of air pollution control stations in Pasir Gudang. These stations are to measure the number of pollutants that were air pollutant parameters being considered in this study which is Particulate Matter (PM_{10}). And also, the difference of date from satellite image will be to determine the pattern of air quality with insert before, and during COVID-19.

ERDAS imagine version 2013 software has been used for other image analysis tasks and the air pollution data according to the parameters chosen will be map using ArcGIS software which is by using a regular map that will be used. The air pollutant of particulate matter was being taken from different algorithm model that will be used to produce the map for the input result.

1.6 Expected Outcomes

The flowchart of the methodology is designed in figure 1.1 that shows the outcome and expected to be from selected the study area, top-rated monitoring station places and processing that users can be throughout and access. The expected outcome that desired are;

i. This study is to measure the air pollutants monitored at three monitoring stations in the south of Johor, Malaysia and the prediction of pollutant concentrations such as particulate matter PM_{10} using satellite images in each monitoring station
ii. The values of pollutant concentration that can determine the changes of a pattern of air quality insert before, during and after COVID-19
iii. The value of air pollutants monitored will be interpolated by Ordinal Kriging to show the map of the distribution of the selected pollutant concentration.

CHAPTER 2

LITERATURE REVIEW

2.1 Introduction

This chapter discusses technologies in air quality monitoring and it is also related to COVID-19 that is affecting Malaysia this year. Besides that, in this project are measures some parameters that contribute to the pollution are described. Thus, all the relevant previous study is discussed and the formulas that have been used for the research such as this are elaborated in this chapter.

2.2 Air Pollutant Concentration

The API consists of five parameters including Carbon Dioxide (CO), Nitrogen Oxides (NO_2), Sulfur Dioxide (SO_2), Ozone (O_3) and Particulate Matter PM_{10} but in this study there were only being considered which is PM_{10}.

2.2.1 Particulate Matter

Particularly referred to as a liquid or solid matter particle that is floating in the atmosphere. The particle size is straightforwardly related to its ability and may cause a health issue (Wikipedia, 2020b). Particles with a diameter of 10 micrometers or less are concerned with the United States Environmental Protection Agency (EPA) because of the particles that typically move through the mouth and nose and enter the lungs. Serious health problems caused when someone inhaled these particles where it affects the heart and lung. Due to their ability to avoid the natural defenses of the respiratory system and to lodge deep in the lungs causing respiratory disease, heart attacks and premature death of particulate matter are considered to be the most harmful form of air pollution. Once, for premature death globally, ambient particulate matter ranks as the sixth leading risk factor (EPA, 2005).

Seohui Park, 2018 stated that for effective management of public health risks, the monitoring and assessment of PM10 and PM2.5 are very important. Urbanization and industrialization have had a negative impact on air quality in this region since East Asia is now increasing prevalence and urbanization due to its rapid economic development. Temporal exposure to elevated PM2.5 concentrations raises the risk of myocardial infarction MI after a few hours in a high-risk population because smaller PM2.5 particles tends to penetrate the cells passively, whereas larger particles are absorbed by macrophages due to the safety of PM2.5 is more harmful than PM10. For a rise of 10 μg / m3 I PM2.5, the risk increased to 4.6 and 8 per cent for all-cause cardiopulmonary and lung cancer mortality, respectively (Thongplang, 2020).

Man-made and natural sources are where the forms of particulate matter can originate. Some sources occur naturally from mold, volcanoes, pollen, forest fires and sea-salt. They are harder to control as they are natural occurrences and are usually left unregulated. Man-made practices include the combustion of fossil fuels in open-fire engines, and various industrial processes. PM10 is most synonyms with road dust, and construction activities. Alternatively, PM2.5 is quite correlated with fuel combustion, industrial products of combustion and vehicle emissions (Thongplang, 2020)

According to (Thongplang, 2020), increasing perception of PM10 and PM2.5 is specifically correlated with possibly harmful effects on human health. According to the World Health Organization (WHO)(WHO, 2018), Particles kill thousands of people worldwide than any other pollutant. Reaction is important because the length of exposure is also a major factor to be weighed, because even short-term exposure to particulate matter may have adverse effects on the human body. The numerical guidance and interim target values are intended to represent concentrations at which increased mortality responses due to PM air pollution are predicted.

2.3 Air Pollution and COVID-19

According to (Gardiner, 2020), it is suspected that air pollution is likely to trigger the effects of COVID-19, in addition to the large range of health harm it causes on its own. Every year, around seven million people around the world have been killed for lung

and respiratory diseases, diabetes, cancer and heart disease caused by air pollution. Higher mortality rates are between 700 per cent and 1,400 per cent higher for those who have contact with COVID-19. Almost 20 % of cases where COVID-19 enters the respiratory system target lung cells become serious. Antibiotics cannot help combat because COVID-19 pneumonia will ensure and is more severe than "normal" pneumonia, because it occurs in all areas of the lungs, and is not caused by bacteria.

Places with worse air quality are more prone. Based on (Love, 2020), Italy was used to hardest hit area with deaths from COVID-19 since Italy's air is worst in Europe. People in Wuhan, China, protested air pollution six months before becoming the first death area for COVID-19. Studies show people living in regions with cleaner air is less likely to die from the previous SARS coronavirus compare to those people who live in places with moderate air pollution with 84 percent chance. Japan, Thailand, Singapore, and Malaysia, are parts of Asia that spreads by the pandemic.

The first cases of COVID-19 were identified in Malaysia on 25 January 2020. Since then, the number of cases has continued to increase, especially in March 2020. Several measures have been called for, including the establishment of a monitoring system for the immediate detection of cases, cause of the symptoms, instant isolation and rigorous case monitoring, and a quarantine of close contacts of those tested positive for COVID-19 since the escalating outbreak of COVID-19 in Malaysia. The Malaysian Government has declared the implementation of the Movement Control Order (MCO) in order to isolate the cause of the outbreak of COVID-19.

COVID-19 has pushed the world economy to a near end as a pandemic spread across the globe. A substantial body of evidence indicates that short-term improvements in air quality have had a significant impact on heart attacks, strokes, and emergency department visits, in addition to the accumulated effects of breathing dirty air for years. If pollution is on the rise, everything increases. The response initiative analyzed the socio-economic health effect of the pandemic on Malaysia as part of the Think City Analytics Group in 2020. According to (Khairuddin, 2020), the Movement Control Oder (MCO), which began on 18 March 2020, shows that maps of nitrogen dioxide have been released to the public to shed some light on the positive effects.

Decreases are definitely only temporary, but to provide cleaner air in the longer term means turning to renewable energy and transport, and not forcing people to stay at home at a dramatic economic expense. If we reduce our consumption of fossil fuels, cleaner pandemic skies demonstrate how rapidly we can minimize emissions.

2.4 Air Pollution Sources in Pasir Gudang

It can be said that the most important contaminants in the major city of Pasir Gudang are nitrogen oxides (NO2), sulfur oxides (SO2), suspended particulate matter (PM10 and PM2.5), and carbon monoxide. There are many factors involved in air quality in Pasir Gudang, the most important of which are geographical factors. Moreover, owing to the dramatic economic development in the Iskandar area in the south of Johor, worries about bad air quality would soon arise. The industrial area of Pasir Gudang is one of the five focal points of growth in the Iskandar district. The Malaysian Government has begun several efforts to improve people's quality of life. Growing public perception of the adverse effects of air pollution drives decision-makers to include air pollution control measures as an important part of environmental development.

2.4.1 Industrial Pollution

The immense expansion of the industrial sector is indeed responsible for emissions pollution. According to this report, there are around 188 industrial areas in Malaysia. Pasir Gudang is one of the fast-growing economic areas that has been recognized as an industrial zone. The rapid growth of industrial areas in Pasir Gudang has resulted in an increase in the population of Pasir Gudang, which has now reached 335,982 inhabitants and has an area of 31,132 hectares. In many industries, however, mounted air quality control systems are found in idle conditions that contribute to the release of contaminants directly into the environment without any filtration (Savira & Suharsono, 2013). Furthermore, the building of short chimneys often limits the release of polluting gases into the upper layers of the atmosphere. One of the main causes of air emissions in Pasir Gudang was fuel burning by both large and small factories. For example, a chemical plant was found with high toxic gas emissions such as methyl mercaptan,

acrolein, and acrylonitrile, which caused a number of students to fall ill and forced hundreds of schools to close. Unfortunately, much of the development has been observed in pollution-intensive areas and industries (Straits, 2021)

2.4.2 Vehicle Pollution

The increase in the number of cars on the road as well as the unregulated discharge of toxic smoke also impacts the condition of the atmosphere due to air pollution. Studies have found that 50% of overall air emissions come from vehicle use. Data also indicates that the 'idle' motor, which is a condition where the engine is switched on but the car does not move, is capable of releasing twice as much petrol (Nurol, 2015). Generally, petrol-driven vehicles such as cars and motorcycles, scooters, etc. use a more powerful four-stroke engine that emits more unburnt fuel and carbon monoxide, whereas diesel-powered cars, such as buses and lorries, emit more soot and nitrogen oxides. Scooters, motorcycles, mopeds, and so on that operate on two-stroke engines using gasoline mixture with lubricant oil emit large quantities of unburnt oil and, as a result, emit large quantities of unburned gasoline in addition to carbon monoxide and soot. Malaysia, as a nation witnessing rapid proportional growth and economic expansion, should be prepared to solve the problems of traffic congestion and driver waste patterns by putting this problem at the center of attention.

2.4.3 Disposal of Toxic Waste and Untreated Industrial Waste

Disposal of hazardous waste and untreated industrial waste from industries creates contamination in the water. The effects of hazardous waste and untreated industrial waste cause the consistency and degree of water sanitation to be compromised and contribute to a variety of diseases as used by individuals in daily life. Aquatic life (fish) in the river is also impaired, which can lead to death due to chemical contaminants found in toxic waste. The problem of chemical waste contamination in the Kim-Kim River, for example, is the unregulated dumping of chemical waste thus dangerous chemicals are exposed to wind and rain, untreated airborne contaminants may have dispersed and harmed smoke inhalers. While the incident is seen as a very valuable

lesson for all sectors engaged in pushing the Malaysian economy to comply with the rules set (Projek & Tepat, 2021).

2.5 Air Pollutant Index API

Refer to the Department of the Environment, DOE, 1997, the concentration limits for selected air pollutants that could adversely affect the health and well-being of the general public are defined in a set of guidelines for air quality, referred to as the Malaysia Recommended Air Quality Guidelines (RMG) for air pollutants (DOE, 1997). The API Air Pollutant Index or, in Malay are called the IPU (Pencemaran Udara input) data air quality in Malaysia (APIMS, 2018). The components of the pollutant index, including carbon monoxide, nitrogen dioxide, sulfur dioxide, ozone and particulate matter PM10, are recorded in ppmv (DOE, 2013).

The API reading determines the dominant air pollutant at the highest concentration. API reading of more than 300 is considered to be dangerous, 200 to 300 is considered to be very unsafe, 100 to 200 is considered to be unsafe, 51 to 100 is considered to be mild, and 0 to 50 is considered to be as good as shown in Figure 2.1. Index values can also be defined as air pollutant levels below the prescribed norm, or levels that indicate warning conditions, emergency and significant damage (DOE, 1997).

As a consequence, the air quality standard was tracked 24 hours a day from the remote air quality control station to assess the human health impacts of various air contaminants, reflecting the duration of intervals to be assessed and registered. As such, in the case of air quality guidelines or guidance, air pollution indexes are typically measured and reported at the same average time as those before. In addition, meteorological data such as surface temperature (C^{o}), wind speed (m/sec), and humidity (%) were also tracked from this air quality station (DOE, 1997).

This study will focus only on three parameters of air pollutant concentrations of the PM10. The Recommended Malaysia Air Quality Guidelines RMG, which contain the 24-hour and 1-hour average period for both particulate matter (μg / m3) originated from the Department of Environment (DOE) automated air quality monitoring stations and will be provided in Table 2.1.

EPA Air Quality Index	Levels of Health Concern	Cautionary Statements	
		$PM_{2.5}$	PM_{10}
0 - 50	Good	None	None
51 - 100	Moderate	None	None
101 - 150	Unhealthy for Sensitive Groups	People with respiratory or heart disease, the elderly, and children should limit prolonged exertion.	People with respiratory disease, such as asthma, should limit outdoor exertion.
151 - 200	Unhealthy	People with respiratory or heart disease, the elderly, and children should avoid prolonged exertion; everyone else should limit prolonged exertion.	People with respiratory disease, such as asthma, should avoid outdoor exertion; everyone else, especially the elderly and children, should limit prolonged outdoor exertion.
201 - 300	Very Unhealthy	People with respiratory or heart disease, the elderly, and children should avoid any outdoor activity; everyone else should avoid prolonged exertion.	People with respiratory disease, such as asthma, should avoid any outdoor activity; everyone else, especially the elderly and children, should limit outdoor exertion.
301 - 500	Hazardous	Everyone should avoid any outdoor exertion; people with respiratory or heart disease, the elderly, and children should remain indoors.	Everyone should avoid any outdoor exertion; people with respiratory disease, such as asthma, should remain indoors.

Figure 2.1 API Status Indicator (Source; Air Quality Air Index, 2019)

Table 2.1 Ambient Malaysia Air Quality Guidelines (Source; New Malaysia Ambient Air Quality Standard. 2020)

Pollutant	Averaging Time	(µg/m3)
Particulate Matter with the size of less than 10 microns PM_{10}	1 Year	40
	24 Hour	100

2.5.1 Calculation for API

Air Pollutant Index (API) is an indicator of air quality status in any specific region. According to the Malaysian Air Pollutant Index, 2018, DOE stated that the sub-index value (sub-API) for six air pollutants included in the API was first determined using the sub-index feature for air quality data obtained from Continuous Air Quality Monitoring Stations to determine the API for a given time span. Appropriate air quality data subject to necessary quality control and quality assurance procedures shall be used before the sub-index is determined (DOE, 1997).

According to (Chooi & Yong, 2016), calculation of the API is also based on the Pollution Standard Index (PSI) accepted at international level by the United States Environmental Protection Agency (USEPA). This method, which is also adopted by the US PSI system, is widely pursued by other countries in an attempt to facilitate a standardized and comparative API system. However, the equation adopted from the Department of Environmental Malaysia will be used to calculate PM_{10} whereas the equation adopted from USEPA from the United States and Pollutant Standards Index (PSI) to calculate $PM_{2.5}$. Generally, higher count reading will be provided if the API reading is based on the $PM_{2.5}$ parameter compared to the API which is based on PM_{10}.

According to the Malaysian Air Pollutant Index (APIMS, 2018), the following is a description of the procedures involved in the measurement of the API values shown in Figure 2.2;

i. Continuous air quality data for the six air pollutant parameters in the API system for a sufficient average time period.
ii. The average concentration of each pollutant over a specified time period is then calculated using a common mathematical method to produce a non-unitary value called a sub-index.
iii. Every pollutant produces the sub-index, and the largest relative sub-index is called API reading.
iv. Record the API at a given time for the preceding average of 1-hour,8-hour or 24-hour specific endpoint for all contaminants with the highest sub-index value obtained using the formula; i.e. API= MAX [Sub-indices of all pollutants]

v. State the particular air pollutant responsible for the importance of the API as the primary parameter along with the index

vi. State the related category of health effects of the API reported

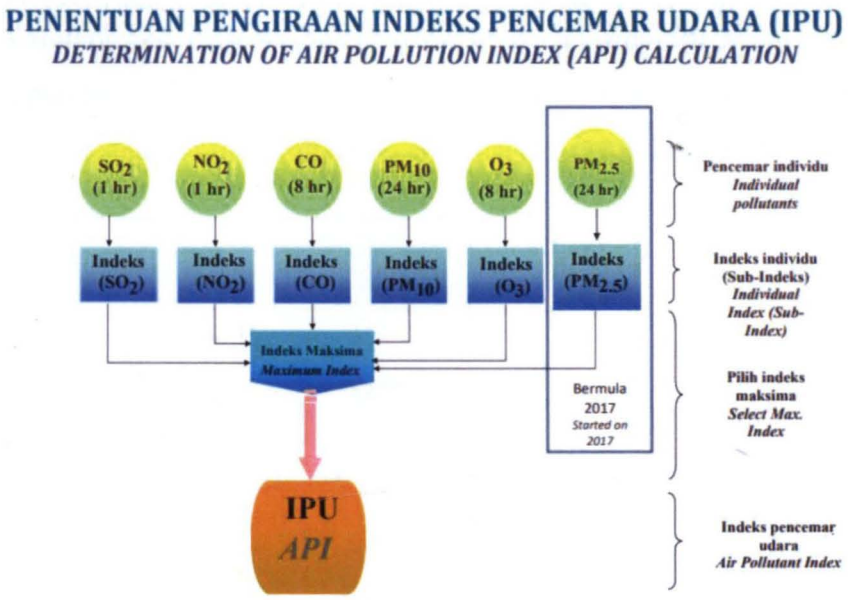

Figure 2.2 Calculation of Air Pollutant Index (Source; APIMS, 2018)

2.6 Continuous Air Quality Monitoring (CAQM)

In 1995, Ambient Air Quality monitoring was privatized and Alam Sekitar Sdn.Bhd (ASMA). A 22-year concession for the planning, development, service and management of a network of 52 continuous air quality monitoring stations has been given to ASMA. CAQM stations are built to continuously monitor ambient pollution for gaseous contaminants with SO_2, CO, NO_2, O_3 and particulate matter (PM_{10} and $PM_{2.5}$) as well as a few meteorological parameters, including distance, wind, temperature, UVB (ASMA, 2015).

In able to locate any potential air pollution issues that may be harmful to human health and the climate, these monitoring stations are primarily situated in metropolitan, traffic and industrial areas. According to (Hasfazilah Ahmat*, 2019), there is a large amount of air pollution, since both testing stations are geographically placed in fast-growing

urban areas. The location of the CAQM in Peninsular Malaysia and East Malaysia is shown in Figure 2.3, respectively.

CAQM is programmed to consistently receive or measure data over the entire data collection period. Figure 2.4 illustrates how CAQM normally contains an instrument for both pollutant and meteorological parameters; an aid instrument (gas supply, testing equipment); a sheltered instrument (temperature-controlled enclosures) and a data collection system for data collection and analysis (Mohd Zamri Ibrahim, 2016).

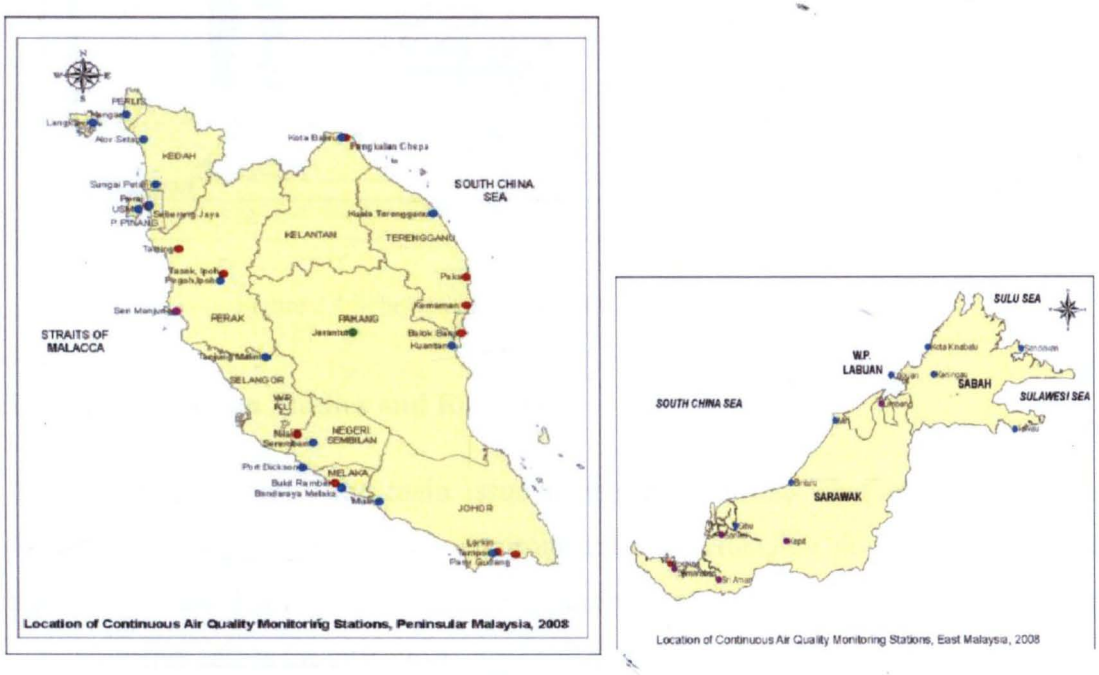

Figure 2.3 Air Quality Monitoring Station in Malaysia (Source; DOE, 2008)

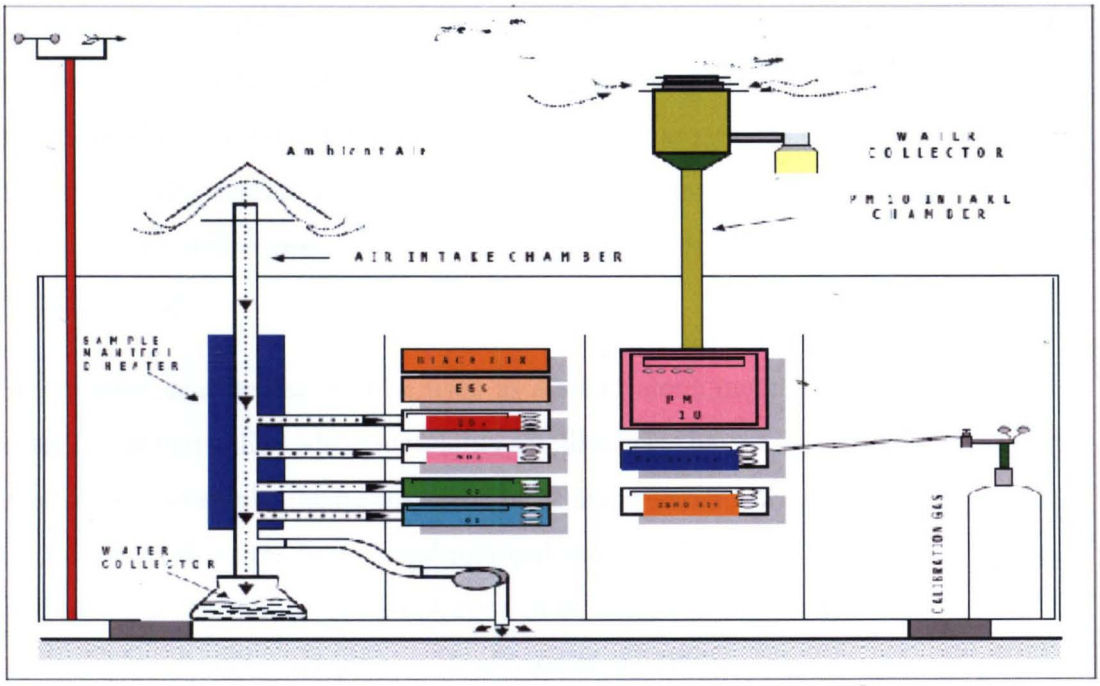

Figure 2.4 Schematic Diagram of CAQM (Source; Google)

2.7 Air Pollution Studies and Reviews

Air quality is currently the main issue in many countries, whether developed or developing. Following day-to-day environmental activities, air pollution has been a big issue today. They cannot produce a decent spatial distribution of air pollutant measurements across the city due to costs and a limited number of air pollutant stations in each location. (Lim et al., 2010) High distribution of air pollution in space can be achieved by satellite observation. In this project, we used the layout mapping in ArcGIS and using data measuring concentration of PM_{10} on different algorithm model, and therefore the data was used to map the distribution of air pollution. Remote sensing allows it to gather data on dangerous or inaccessible area or remote locations.

2.7.1 Importance of the Remote Sensing

Based on USGS, 2020 the detection and monitoring of the physical characteristics of the area is reflected and the radiation emitted at a distance typically from the satellite or aircraft is a process that occurs from remote sensing. It can be used by aircraft, spacecraft, ships or satellites for recording devices such as camera, laser, radar, sonar

seismograph, gravimeter, etc. Here are some examples of satellite cameras and aircraft taking photos of large areas on the surface of the earth. This makes it possible by seeing much further than this can stay on the deck, the sonar systems on ships are often used to produce photographs of the ocean floor without having to go to the bottom of the sea, and the satellite camera is used to take pictures of changes in ocean temperature (USGS, 2012).

Air quality satellite data can be used as a stand-alone method, such as the effect of satellite data on policy where air quality satellite maps have a direct influence on policy makers. For example, the tropospheric NO2 maps across Europe have managed to put air quality high on the Netherland national issue. Satellite data maps show the global and regional distribution of air pollution in an objective manner and place the national situation in a broader perspective (Veefkind et al., 2007).

Next, remote sensing was also used to inform the general public of the air quality current situation and even in the previous era by means of publicly available satellite maps. For instance, in the help and guidance of housing and/or holiday decisions, people who are oversensitive to air pollution can have these maps. In order to provide reasonable coverage, the strategic plan of ground-based measurement sites with high spatial resolution of air quality satellite data is helpful in analyzing the number of ground-based measurement sites required. Satellite data may also display unique characteristic that need to be investigated in field campaigns (Veefkind et al., 2007).

In addition, remote sensing can display the spatial distribution of pollution as the geographic variations in the emission databases can be checked by analyzing the time-average satellite map of pollutants. A resolution of 10 x 10 km2 or better is required for these charts, but is not possible from ground-based nitrogen dioxide networks. One benefit is the fluctuations in pollution inventories that can be checked with long-term satellite data archives, but can also be accomplished by utilizing ground-based knowledge (Veefkind et al., 2007).

2.7.2 Air Pollution Mapping Using Remote Sensing Data

According to (Lim et al., 2010), environmental pollutant applications such as water quality and air pollutants was widely used by using remote sensing techniques. Further satellite data were used for environmental atmospheric studies such as NOAA-14 AVHRR and Landsat TM. Nevertheless, their large spatial range and precise repetitive measurements provide another useful tool for monitoring aerosol and traffic movements, which is why the satellite picture has been used. Surface reflectance is the essential to the detection of atmospheric components from remotely sensed data. This may change the frequency of the signal by dispersing the absorption process and its path by this means (Sifakis & Deschamps, 1992)

Satellite observations of the Earth's surface in the solar spectrum have an influence on the environment, so that the signal measured by the satellite sensor is the amount of the Earth's and Atmospheric impacts. Tropospheric aerosols have a major impact on Earth's radiation budget, but quantification of radiation changes is challenging due to atmospheric aerosol concentrations that vary widely in quality, scale, volume, and time (Buseck, P. R.; Schwartz & It, 2021) . Depending on their form, suspended aerosols have a direct and indirect impact on local, regional and global temperatures, creating a cooling or warming effect on the earth, at the aerosol layer altitude and at the top of the atmosphere(Iwona S. Stachlewska, Olga Zawadzka, 2007).

According to (Lim et al., 2010) said the smoke haze is linked to a category of contaminants called aerosols, liquids or solid particles released to pollution from natural or man-made sources. Aerosol particles have an impact on the climate. During the 1990s, the average temperature of the atmosphere has increased by 0.6 ^{o}C and has exceeded its maximum level over the last centuries. This accelerated change in temperature is due to a transition of less than 1% in the energy balance between the absorption of incoming solar radiation and the release of thermal radiation from the planet. Becomes if the radiant energy absorbed and emitted by the Earth shows a sign of the Earth's atmosphere and surface properties by measuring the wavelength, angular and polarizing properties of the radiation, thus the potential of satellite sensors to quantify certain atmospheric and surface characteristics.

Nonetheless, according to (Basly, Ludovic, and Baleynaud, 2020), mapping efficiency is highly needed due to the following major benefits;

- To provides a detailed overview of the city
- Presents the main causes of pollution and their extension
- This indicates that it is easier to make efforts to raise the amount of pollution
- Allows to further explore the connection that could occur between city features and the distribution of air pollutants;
- This shows that it is better to make efforts to raise the amount of pollution
- Helps to further examine the relationship that may exist between city features and the distribution of air pollutants
- It serves as a foundation for improving the sampling strategy by transferring some stations to suitable locations, or by adding some or possibly eliminating some of them

2.7.3 Conventional Method

Meer, 1991, knowledge provided by remote sensing the earth's surface from aircrafts is not easily obtained by surface observation. Till previously, the main drawbacks of remote sensing was how information on the subsurface cannot be accessed and that surface information appears to lack precision. Traditional scanner e.g. Landsat MSS and TM, as well as SPOT, obtain information in a few separate spectral bands of various widths, thus filtering the reflectance characteristics of the surface to a large extent. Therefore, in order to cope with the increased amount of data, new types of scanners have been developed with high spectral resolution, resulting in a new image processing technique (MEER, 1991).

Gupta, 2009, four phases of the conventional approach to air quality status planning, namely monitoring, modeling, planning decision-making and, finally, implementation, are generally achieved. Monitoring air pollution is achieved through the three mechanisms for monitoring air pollution that are being achieved, namely integrated sampling, sampling and passive sampling. Previous studies towards contact measurement, integrated path measurement, simultaneous analysis, fence-line and flux

measurement, and the conventional approaches to assess the pollution level are not efficient. It also is does not efficient towards global measurement (Gupta, 2009)

Remote-sensing air monitoring equipment has been found to be capable of determining the level of air pollution in the target region, which could be more useful to the planning of air quality level. The traditional air pollution models, which forecast various parameters, such as meteorology, traffic volume, developmental status, etc., provide the expected data for non-spatial information. Such efficiencies can be enhanced by developing remote sensing technologies.

Geographic information system GIS, using spatial records for a safer, more reliable and cost-effective approach to air quality status planning. Various GIS capabilities may be used in air modeling, including the placement of monitoring stations, the development of pollution control systems and the construction of a space decision support system. The output of the pollutant data in the form of spatial data can be obtained by modeling the air quality in the GIS method. GIS software are able to support the development of geospatial air quality models (Dr. I.C. Agrawal, Dr. R.D. Gupta, 2003)

2.7.4 Application of GIS in Air Pollution Studies

According to Kirti Bhandari, GIS is a computer-based method for identifying and evaluating existing geographical phenomena and occurrences on Earth in 2009. GIS software combines standard database processes like query and statistics with specific map visualization and spatial analysis advantages. Such features distinguish GIS from other data systems to make it convenient for a wide range of public and private agencies to explain events, predict outcomes and plan their strategies.

In fact, the GIS offers data collection, data processing, data interpretation and analysis and presentation of findings in both graphic and report formats, with a special emphasis on the preservation and use of the inherent qualities of spatial data. The process of integrating, organize, interpret and respond to spatial questions is a unique characteristic of geographic information (Sharma et al., 2015)

Several efforts have recently been made to map the distribution of related pollution and to determine the pattern of pollution in the GIS research area. Through the advent of GIS and geostatistical techniques, a broad variety of spatial interpolation techniques has become accessible. These are divided into broad methods which, based on the entire sample data and local methods, include moving window methods, kriging, spline interpolation where a number of local predictions are based on the nearest data points (Briggs et al., 2010)

A number of these interpolation methods have established applications for pollution modeling, but mostly on a fairly small regional scale. Kriging in its various forms has been used to map national pattern of Nitrogen Oxide (NO2) concentrations, acid precipitation and ozone concentration, and to help design continental-scale monitoring network also report the use of kriging to estimate and map exposures to groundwater pollution and microwave radiation (Briggs et al., 2010).

In comparison, the density and distribution of most of the monitoring networks is typically low. As a result, the current monitoring network offers only a small image of the spatial pattern of air pollution, potentially skewed patterns forecasts, and inadequate indicators of human exposure. The spatial analysis and overlay technique available in GIS which provides powerful tools for pollution mapping. As GIS monitors pollution parameters consistently and allows spatial analysis to be considered as the most efficient technological tools for questioning (Briggs et al., 2010).

2.7.5 Importance of Geographic Information System (GIS)

GIS is an information system that deals with spatial or geographical coordinate data. The use of GIS spatial data for the analysis of air pollution is a recent technology (Ahmad et al., 2010). Not only does GIS collect, store, evaluate, view geographically referenced information, but this hardware and software device can also retrieve information on demand flexibly. What makes it very effective, however, is the ability to link apparently irrelevant information by using spatial context and also to draw conclusions on the multivariate relationship of this information (Ahmad et al., 2010).

Generally, there is a positional reference to some point or extent on the globe when information about a place is provided. For example, it is crucial to know the geographical background if the Pasir Gudang is located in Johor. Responsible for this is the use of a spatial information database based on a standard position reference system. For example, longitude and latitude, projected cartographically in two or even three dimensions, to perform the best analysis and show spatial results and manipulation (Ahmad et al., 2010).

2.8 Summary of Chapter

After performing research and reviewing the literature, it can be concluded that remote sensing data has become a satellite remote sensing study as a new method for monitoring air quality and is sufficient for use in the measurement of air pollutant dispersion. Its characteristics of satellite data are very complementary to the field network on the ground. It provides detailed, high-resolution measurements of specific locations.

Therefore, all the studies analyzed have been analyzed in order to obtain the appropriate approach that can be used in this analysis. Depending on the availability and requirements of the data, the parameters involved the appropriate formula to be used and the software package required to determine the appropriate method. The next chapter will discuss the process in detail.

CHAPTER 3

METHODOLOGY

3.1 Introduction

This chapter will explain methods used to complete this chapter. All steps and procedures explain the function and discuss some research. The research method of this study can be classified into 3 key operations, which are selection of study area, selection of data collection and data processing. On the selection of study area which are selected the area for make the research over the area. The study area is chosen that covered by industrial and urban area, were suitable for measure air pollution. While for the data collection is from the satellite data that contain the Landsat imagery (Landsat 8) of the remote sensing has been chosen to provide information about the particle of parameter around the study area. The data processing of acquired data that will process in the software to make the comparison of the data and create the map using the ERDAS and ArcMap software.

3.2 Flow of Work

The methodological process comprises several phases such as subset images, making a calculation Conversion from DN to Radian and Radian to TOA Reflectance using spatial model maker, and calculation particulate matter (PM10) using different algorithm models and lastly, mapping the air pollution distribution. The methodological is described in a flowchart shown in Figure 3.1

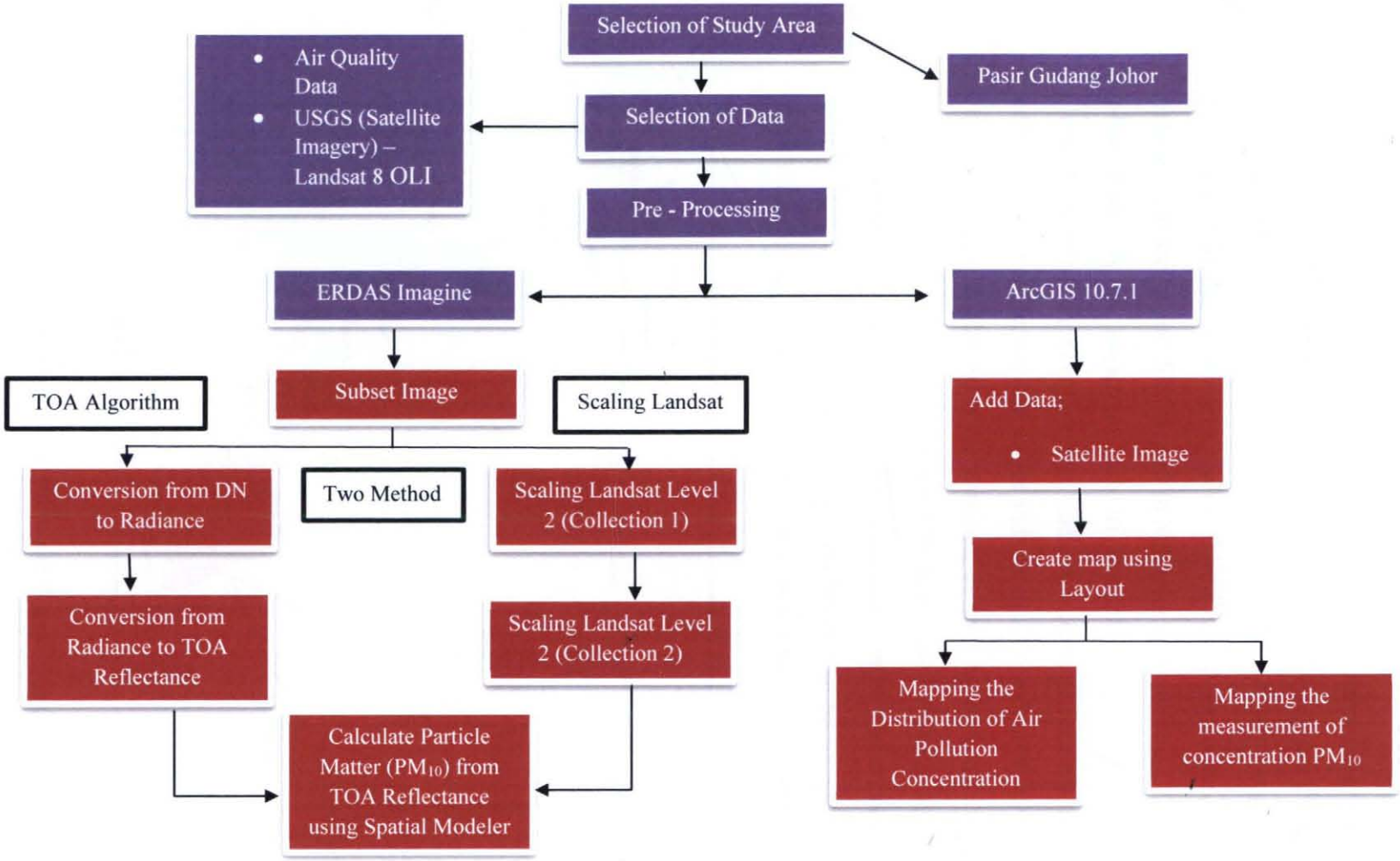

Figure 3.1 Flowchart of Methodology

3.3 Study Area

This study focuses on the issue of air pollution in the Johor Bahru region of Malaysia. Johor Bahru is located in the southern part of the Malaysian Peninsula Figure 3.2. Johor Bahru Latitude; 1◦ 28' 13" N; Longitude; 103◦ 54' 10" E was chosen as the main research site in this study area. Johor Bahru has a population of 497,097 and its metropolitan area is the third largest in Malaysia and covering 220 km2 of study area. Johor Bahru is an important hub of manufacturing, logistics, and commerce. Electronics, petrol chemical, capital, and petrochemical refinery and shipbuilding, as well as tourism industries are major industries. The industrial town near Johor Port was the world's largest palm oil terminal, as well as Tanjung Langsat Port, which handles bulk cargo such as liquefied petroleum gas and other chemical substances. Pasir Gudang, Skudai, Senai, and Kulai are heavy industrial areas located east of the metropolitan area. This location is selected because of its location near the industry where the most air pollution-prone region is possible.

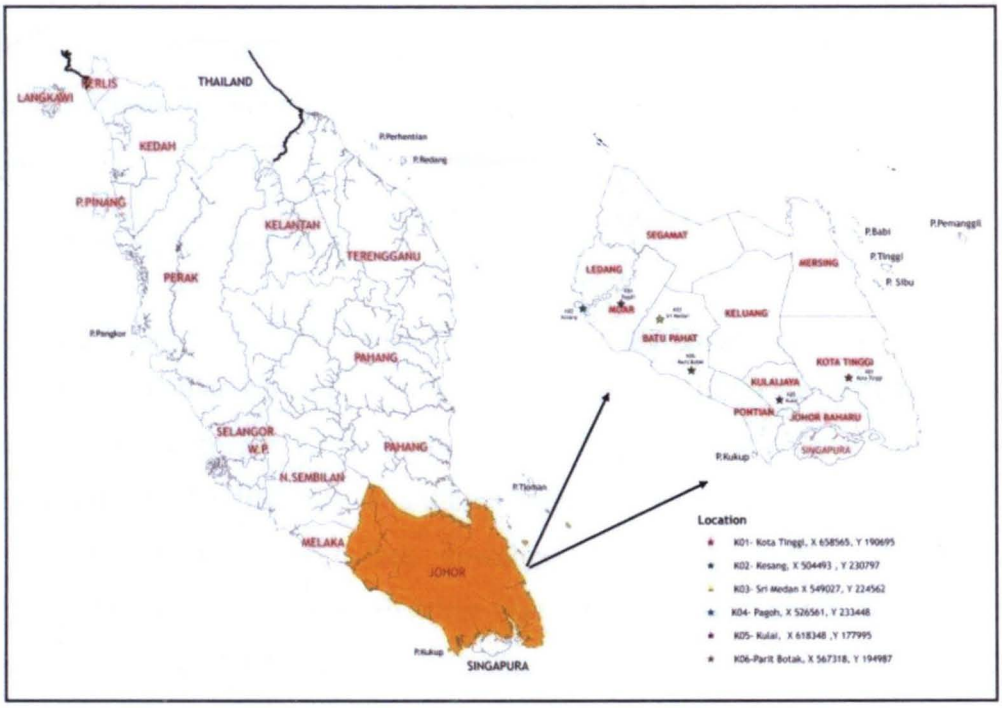

Figure 3.2 Johor Bahru area (Source; Goggle, 2019)

3.3.1 Selection of Air Quality Monitoring

The Department of Environment (DOE) continuously tracked the ambient air quality using their network of monitoring stations. There are 52 continuous monitoring stations in Malaysia, but in this analysis the monitoring station focuses only on two stations, as shown in Table 3.1. It is situated geographically in both the residential and industrial areas. In this study, the monthly dataset which selects only three dates is 10 March 2020 and 26 March 2020 (DOE, 2020)

Table 3.1 Location of Air Quality Monitoring in Johor

Station ID	Location	Area Category
CA	Sekola Menengah Pasir Gudang 2	Industrial

3.4 Data collection

There are three types of data used in this research, the primary data collected from the U.S. Geological survey (USGS), Department of the Environment (DOE) reports on air quality and topographical info. Such requirements provide data quality and compliance with remote sensing and GIS technologies, and data quality focused on air emissions studies.

1) Remote Sensing Data

The primary data used in this analysis is satellite image of Landsat 8 OIL. This data is used as the main data which processes the image in order to see the distribution of air quality. Only two images dated 10 March 2020, and 26 March 2020, were selected in this study due to the difficulty in getting a cloud free scene over the study area. U.S. Geological Survey (USGS) free download of remote sensing data website (http://earthexplorer.usgs.gov). The data was selected as Landsat 8 Level-2 where, dates of 10 March 2020 are collection 1 and 26 March 2020 are collection 2. In addition, this analysis considered only images of less than 10 percent cloud cover, since one of the key problems in these regions is the presence of a high cloud density. Only 40 percent of remote sensing data was considered according to this constraint.

The remote sensing data to be used in this analysis is from the Landsat image, which is Landsat 8 Operational Land Imager (OLI) images, consisting of nine spectral bands with a 30-meter spatial resolution for Bands 1 to 7 and 9 shown in Table 3.2. For this analysis we used visible bands 1,2,3, and 4 of Landsat 8 OLI picture for the region of Johor Bahru. The Landsat sensor is capable of detecting five images using seven different wavelengths at one time.

Table 3.2 Spectral and Spatial Characteristics of Landsat 8 OLI Bands.

Bands	Wavelength (micrometres)	Resolutions
Band 1 – Coastal Aerosol	0.43 – 0.45	30
Band 2 - Blue	0.45 – 0.51	30
Band 3 – Green	0.53 – 0.59	30
Band 4 – Red	0.64 – 0.67	30
Band 5 – Near Infrared (NIR)	0.85 – 0.88	30
Band 6 – SWIR 1	1.57 – 1.65	30
Band 7 – SWIR 2	2.11 – 2.29	30
Band 8 – Panchromatic	0.50 – 0.68	15
Band 9 – Cirrus	1.36 – 1.38	30
Band 10 – Thermal Infrared (TIRS) 1	10.60 – 11.19	100
Band 11 – Thermal Infrared (TIRS) 2	11.50 – 12.51	100

Air Quality Data

The data on air quality for this study were collected from the Department of Environment, Air Quality and the Ministry of Natural Resources and the Environment of Malaysia. Air quality data refers to the levels of pollution observed at existing ground stations in the air. The data on air quality can be obtained from the Malaysian Department of Environment (DOE) subsidiary Alam Sekitar Malaysia (ASMA). DOE is responsible for the continuous monitoring and measurement of the pollutant on a daily basis. The descriptions of air contaminants included in this study are particulate matter (PM_{10}), particulate matter ($PM_{2.5}$) and nitrogen oxide (NO_2). There are 3 stations inside the sample region for this work and the arrangement is also seen in Table 3.3.

Table 3.3 Air Quality Monitoring Stations

Station ID	Location	Coordinates	
		Northing	Easting
CA	Sekola Menengah Pasir Gudang 2	1° 28' 12.7	103° 53' 36.5

3.5 Selection Software

1) ERDAS IMAGE 2016

The software package is chosen to perform the methodology and to get the results needed. The method used in the survey area was developed in ERDAS IMAGE 2016, where the model creator was the digital image process, the remote sensing data and the derivation of standard deviations. The technique presented in this paper is used for measured the particulate matter and nitrogen dioxide of a given LANDSAT 8 image with the input of the Coastal Aerosol, Red, Green and Blue only was considered in the technique.

2) Geographic Information System (GIS)

While the approach of GIS is also used to map the results and overlay land use maps. GIS tools have become an important component of the methodology for detecting pollution. GIS platform includes the features and software resources required to store, analyze and view geographic and temporal information. According to Khaled Ahmad Ali Abdulla Al Koas, 2010 for space editing, analysis, design, analysis techniques and 2D/3D visualization / outcome. ArcMap enables the user to explore data in the data collection, suitable symbolize features and build maps appropriately. Last result will show the maps created in ArcMap usually include features such as north arrows, scale bars, names, legends, neat lines, etc.

3.6 Data Processing

The data must be processed and analyzed after collection in accordance with the purpose-set outline at the time of the development of the research plan.

3.6.1 ERDAS Process

In ERDAS Software, there are several stages in the processing of satellite images, which are the subset of the study area, the conversion from DN to Radiance, the conversion from Radiance to Reflectance. The next subsection will provide a clear description of the processing step for each stage.

3.6.1.1 Pre-processing

Data pre- processing includes stack layer and subset the image. After that, radiometric correction is applied by converting the DN values to radiance. The DN values of Landsat 8 scenes were converted to top of atmosphere (TOA) reflectance values using the algorithm given. After radiometric correction, the following steps were applied to 1 until 4 images were used.

1) Stack layer

Layer stacking is a method for merging several images into one file using this tool 

. The Landsat 8 OLI picture has 11 wavebands and contains row and column detail. As a result, all Landsat scenes recorded a series of GeoTIFF files with different TIFF files for each of the bands. At the next step, the Landsat bands are unpacked for each image that the images should be of the same scale (number of rows and number of columns), which ensures that the other bands of different spatial resolution are repeated to the target resolution. In other words, all images or bands should have the same spatial resolution so that they can perform layer stacking. The combination of images/bands will however, increase the final stacked image size and hence increase the processing time later in the analysis.

2) Subset Image

The Subset is a Slip method process as well as an image extract process. This phase describes how to cut out a subset of the larger original image in order to simplify the analysis and focus on the part of the scene that is of primary interest. The area for subset image consists only of a study area, including Pasir Gudang and parts of the Johor area. The image that is collected from the USGS is subset using the subset coordinates as shown in Table 3.4.

Table 3.4 Coordinates of subset

Points	Coordinates (x)	Coordinates (y)	Notes
1	375300.00	165030.00	Upper Left
2	380970.00	160770.00	Lower Right

3) Types of Method Calibration

There are two types of method that can be used to calibration the image from USGS which in Landsat 8 Level-1 using TOA algorithm to conversion of DN to Radiance and continues convert from Radiance to TOA reflectance. Besides that, second method which Landsat 8 in Level-2 there have two different scale factor that have to be calculate.

a) TOA Algorithm

i) Conversion of DN to TOA radiance

OLI data can be converted to TOA spectral radiance using the radiance rescaling factors provided in the metadata file. The following equation is used to convert DN values to TOA radiance as Eq.1

$$L_\lambda = M_L * Q_{cal} + A_L \quad (3.1)$$

Where:

L_λ = TOA spectral radiance (Watts/ (m2 * srad * μm))

M_L = Band-specific multiplicative rescaling factor from the metadata (RADIANCE_MULT_BAND_x, where x is the band number)

A_L = Band-specific additive rescaling factor from the metadata (RADIANCE_ADD_BAND_x, where x is the band number)

Q_{cal} = Quantized and calibrated standard product pixel values (DN)

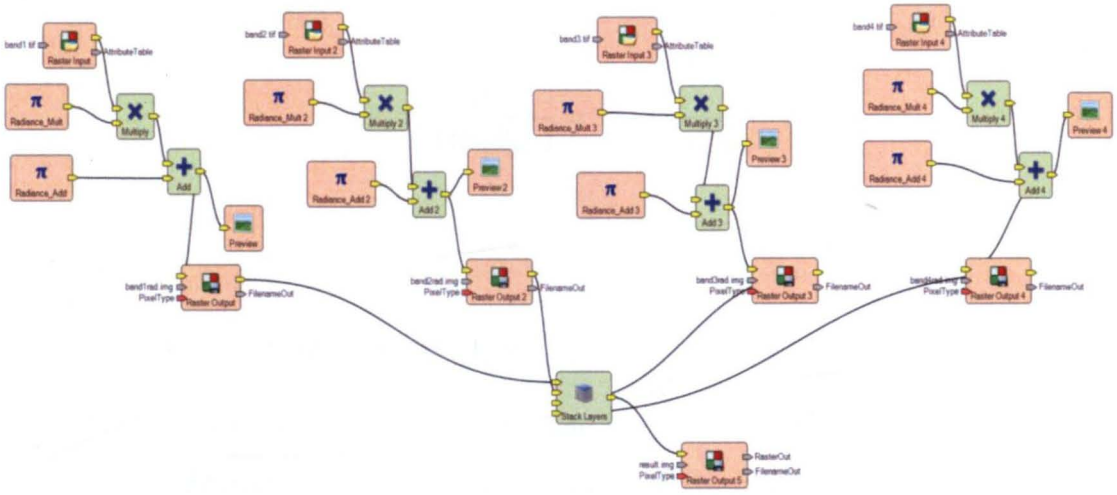

Figure 3.3 Spatial Model to Convert from DN to Radiance

ii) Conversion of TOA radiance to TOA reflectance

After the top of radiance is calculated, the top of atmosphere reflectance (TOA) must be calculated by using an image from top of radiance. OLI band data can also be converted to TOA planetary reflectance using reflectance rescaling coefficients provided in the product metadata file (MTL file). The following equation is used to convert DN values to TOA reflectance as Eq.2

$$p_\lambda = M_p * Q_{cal} + A_p \quad (3.2)$$

Where:

p_λ = TOA planetary reflectance, without correction for solar angle. Note that ρλ' does not contain a correction for the sun angle.

Mρ = Band-specific multiplicative rescaling factor from the metadata (Reflectance_Mult_Band_x, where x is the band number)

Aρ = Band-specific additive rescaling factor from the metadata (Reflectance_Add_Band_x, where x is the band number)

Qcal = Quantized and calibrated standard product pixel values (DN)TOA reflectance with a correction for the sun angle is then:

$$\rho\lambda = \frac{\rho\lambda'}{\cos(\theta_{SZ})} = \frac{\rho\lambda'}{\sin(\theta_{SE})} \tag{3.3}$$

Where:

ρλ = TOA planetary reflectance

θ_{SE} = Local sun elevation angle. The scene centre sun elevation angle in degrees is provided in the metadata (SUN_ELEVATION).

Θ_{SZ} = Local solar zenith angle; $\theta_{SZ} = 90° - \theta_{SE}$

For more accurate reflectance calculations, per pixel solar angles could be used instead of the scene centre solar angle, but per pixel solar zenith angles are not currently provided with the Landsat 8 products.

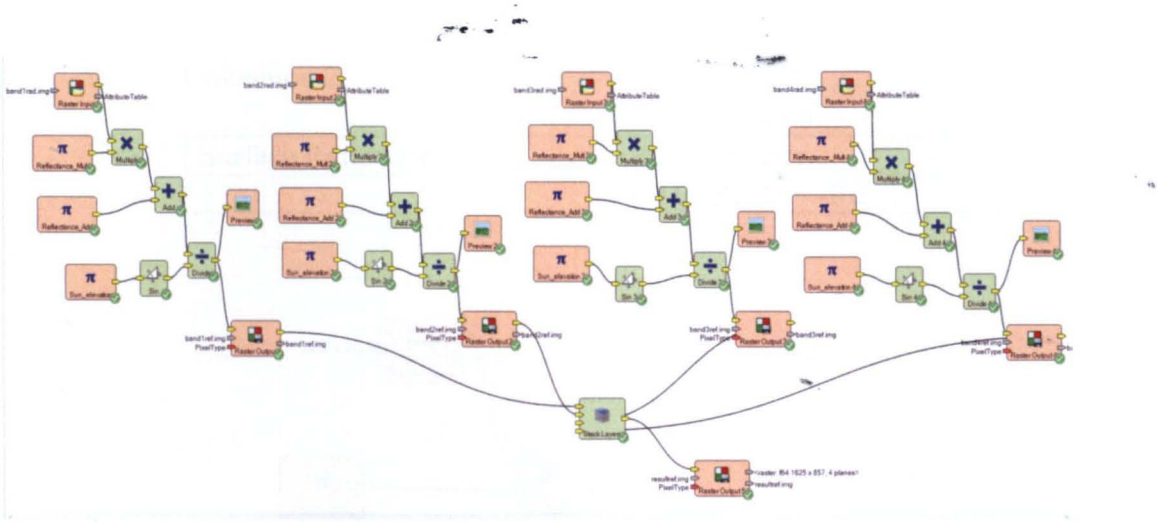

Figure 3.4 Spatial Model to Convert from Radiance to Reflectance

b) Scaling of Landsat Level 2

A scale factor has to be applying in both Collection 1 and Collection 2 Landsat Level 2 surface reflectance before using the data. In this study, image dates of 10 March 2020 are using Collection 1 where 26 March 2020 are using Collection 2. The following will show;

i) Collection 1

Table 3.5 Scale factor of Collection 1

Surface Reflectance	Scale Factor
	0.0001

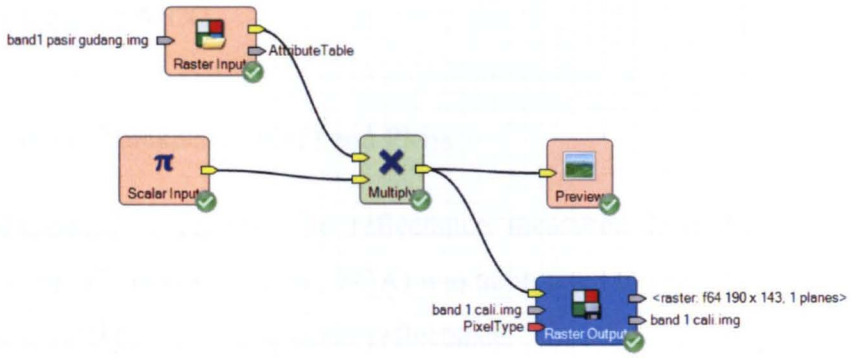

Figure 3.5 Spatial Model to scaling Landsat Level 2 in Collection 1

ii) Collection 2

Table 3.6 Scale factor of Collection 2

Surface Reflectance	Scale Factor
	0.0000275 + -0.2

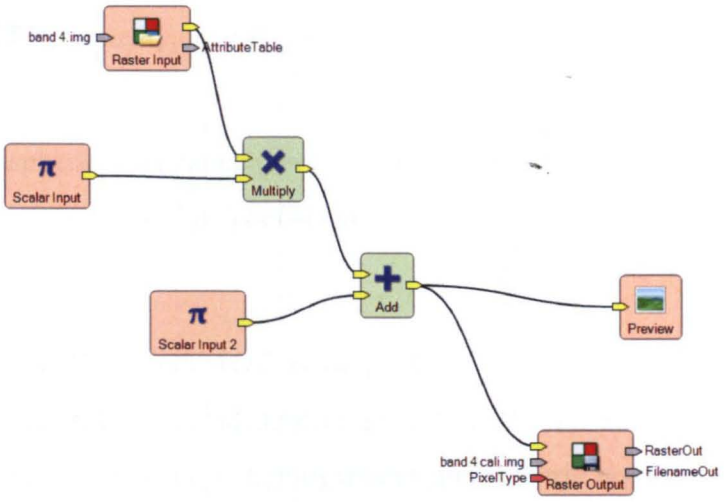

Figure 3.6 Spatial Model to scaling Landsat Level 2 in Collection 2

3.6.1.2 Calculate value of PM_{10}

Following a radiometric correction, the reflectance measured from the satellite (reflectance at the top of the atmosphere, TOA) was subtracted by the amount of the surface reflectance to achieve atmospheric reflectance. The resulting PM_{10} model was used to predict PM_{10} concentrations over Johor at Pasir Gudang Johor, and a PM_{10} map was generated for distribution of particles dated between 10 March 2020 before MCO and 26 March 2020 during MCO.

1) Aerosol Optical Thickness (AOT) and PM_{10}

Following a radiometric correction, the reflectance measured from the satellite (reflectance at the top of the atmospheric, TOA) was subtracted by the amount of the surface reflectance to achieve atmospheric reflectance. The algorithm of AOT for single band or wavelength (λ) is simplified as (Saraswat et al., 2017)

$$AOT(\lambda) = a_o R(\lambda) \tag{3.4}$$

Equation (3) is rewritten into multiband equation as:

$$AOT(\lambda) = a_j R_{\lambda 1} + a_j R_{\lambda 2} + a_j R_{\lambda 3} + a_j R_{\lambda 4} \ldots. \tag{3.5}$$

Where $R_{\lambda 1}$ is the atmospheric reflectance (i = 1, 2 and 3 corresponding to wavelength for satellite), and a_j is the algorithm coefficient (j = 0, 1 and 2) are empirically determined.

The interaction between PM_{10} and AOT is derived from a single homogeneous atmospheric layer comprising spherical aerosol particles. The interaction between PM_{10} and AOT is derived from a single homogeneous atmospheric layer comprising spherical aerosol particles. It can then be expected that the PM parameter would be more explicitly associated with AOT. Using the information collected by the spectral AOT extraction, a system has been developed to retrieve particulate matter concentrations. By substituting AOT in term of PM_{10}, into the equation (5), the algorithm of PM_{10} with spectral reflectance of multi-band wavelengths (λ) is simplified as (Saraswat et al., 2017)

$$AOT(\lambda) = a_j R_{\lambda 1} + a_j R_{\lambda 2} + a_j R_{\lambda 3} + a_j R_{\lambda 4} \ldots. \tag{3.6}$$

Where $R_{\lambda 1}$ is the atmospheric reflectance (i=1,2,3,4.. corresponding to satellite (bands), and a_j is the algorithm coefficient (j=0,1,2,3 ....) are empirically determined.

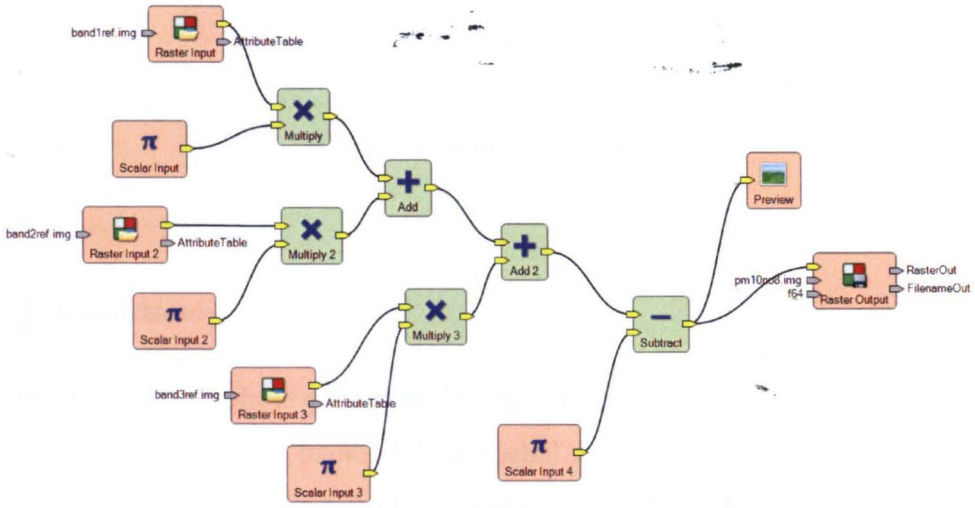

Figure 3.7 Spatial Model to Calculate Particulate Matter (PM10)

3.6.2 Mapping of Air Pollution Dispersion

Mapping of the air pollution is the output for this study which is the last step in this procedure. This step will be using or need to make a layout. A layout is a composition of one or more maps, along with supporting elements, such as a title, a legend, and descriptive text. Some layouts include more than one map. For example, a layout may have a main map and an overview map to show the main map in a larger geographic context. In this way, the distribution of air pollution of Pasir Gudang is can be easily visualized and the factors contributing can be recognized. In the next chapter, the analyses of the results from this chapter will be clearly explained.

3.7 Conclusion

This chapter has explained the selection of the study area, and the data needed in doing this research. The outlines of methodological are explain in details. Besides, the software needed to carry out in the investigation is also described. The output for this chapter is the mapped of the air pollution dispersion. Next chapter, the analyses and results of measurement of PM_{10} using different algorithm will be shown. Besides, the output for this study which is the air pollution dispersion for each algorithm will be displayed therein.

CHAPTER 4

RESUTL AND ANALYSIS

4.1 Introduction

This chapter explains about all the results that have been made during processes in the methodology phase from Chapter 3. The spatial model method was used to calculate PM_{10} concentration from the reflectance values of Landsat 8 OLI visible bands which are applied in this study, results and the illustration of the particulate matter concentrations are discussed. The implementation of interpolating both pollutants data from air quality data and aerosol optical thickness derived from satellite imagery are also discussed from date differencing before MCO and during MCO. The expected results of this study which is a map of air pollution distribution over Pasir Gudang Johor are presented and visualized in this stage.

4.2 Result for Scaling Landsat Level 2

This process is done in the ERDAS Imagine by using the Spatial Modeler tool 

. The formula for the conversion in the previous chapter then applied in the modeler to get the result. In this calculation, there are using band 1, band 2, band 3, and band 4 only. Refer to Figure 3.5 and Figure 3.6 in the previous chapter, there are two collections that have to be done which result for collection 1 shown in figure 4.1 and the result for collection 2 in Figure 4.2.

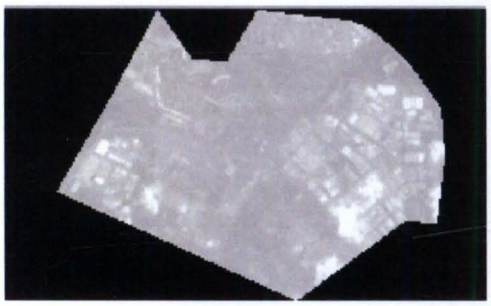

BAND 1

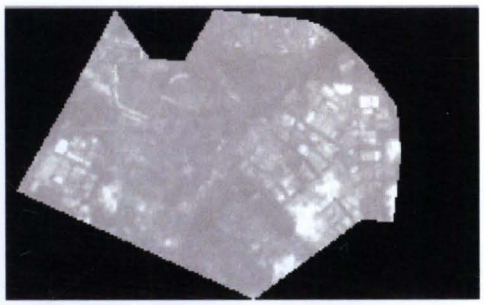

BAND 2

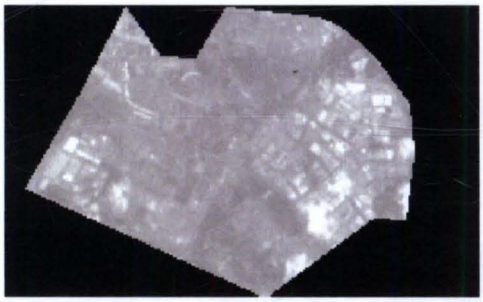

BAND 3

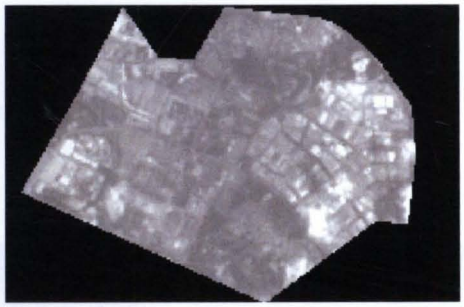

BAND 4

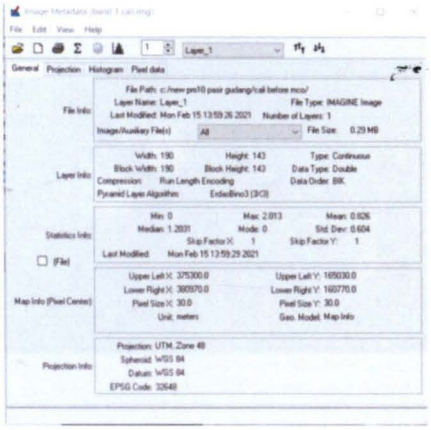

BAND 1

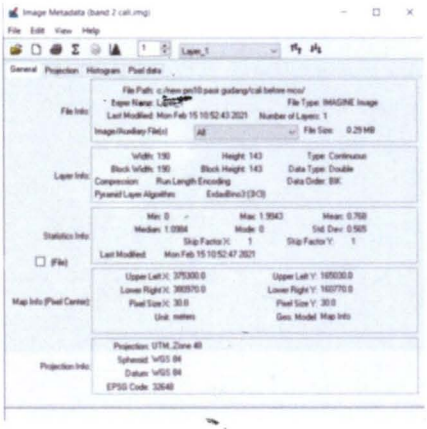

BAND 2

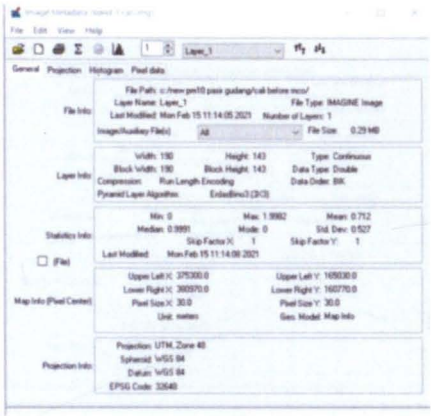

BAND 3

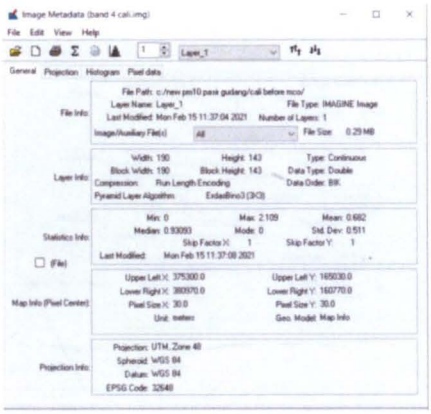

BAND 4

Figure 4.1 Result Collection 1 (10 March 2020)

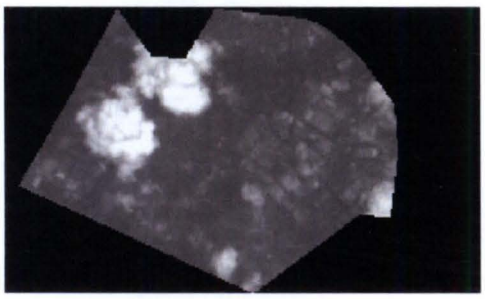

BAND 1

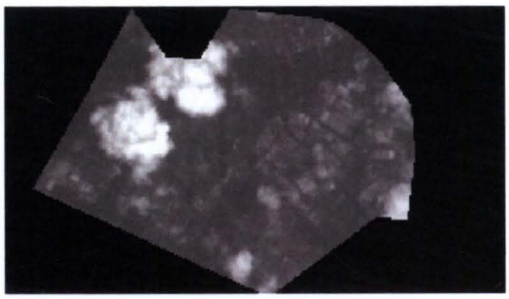

BAND 2

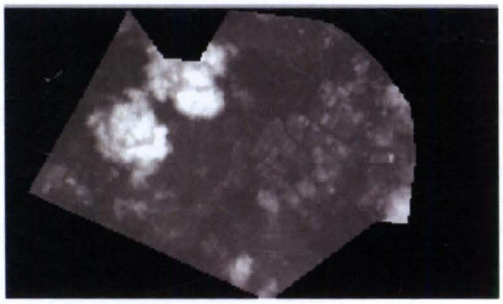

BAND 3

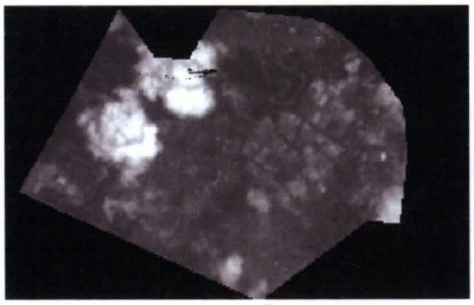

BAND 4

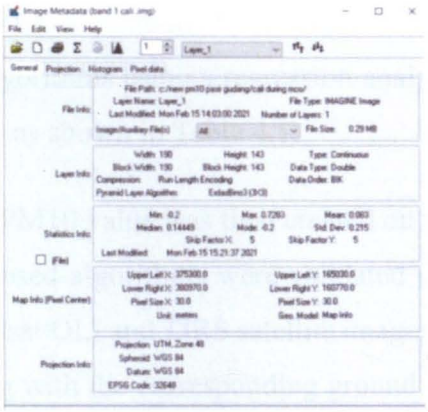

BAND 1

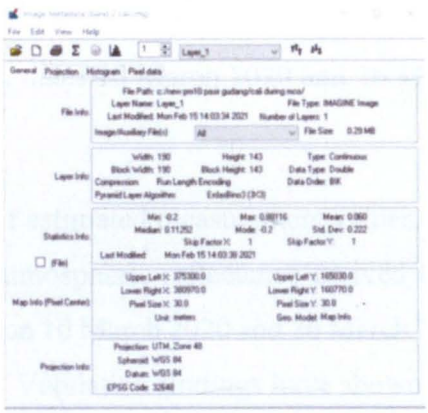

BAND 2

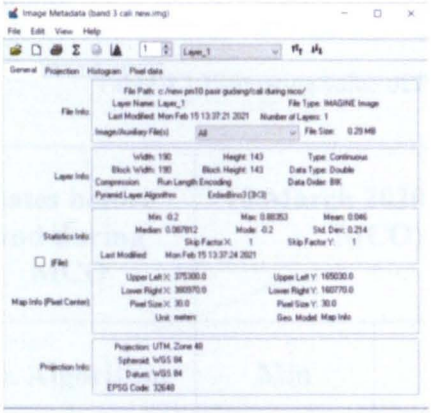

BAND 3

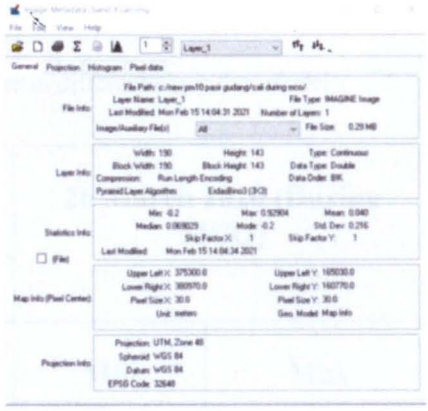

BAND 4

Figure 4.2 Result for Collection 2 (26 March 2020)

4.3 Measurement and modelling of particulate matter concentrations

The statistical findings of the regression models developed are demonstrating how well spatial variance in air pollution can be predicted by applying the various regression models developed. Many of the regression models developed for particulate matter were highly important. Many algorithms have been developed to correlate satellite reflectance and PM_{10} values. These algorithms were used to measure the concentration of PM_{10} from the reflectance values of the Landsat 8 observable OLI bands. Figure 3.5 displays the spatial model used to measure PM_{10} from the Landsat8 OLI reflectance values and the values of algorithm are using from this citation (Saraswat et al., 2017) to doing calculation of PM_{10}. There also show the comparison values of different types of algorithms using a regression analysis in both dates 10 March 2020 and 26 March 2020 as shown in Table 4.1.

The PM10 value was then created on the basis of estimated measurement values. The proposed algorithms were validated using the atmospheric reflectance derived from Landsat OLI and TIRS satellite images acquired on 10 March 2020 and 26 March 2020 along with the corresponding ground truth data. Validation findings have shown that models developed using Landsat OLI and TIRS data are important for particulate matter, while the satellite data described cannot be used to reliably forecast gaseous pollutants.

Table 4.1 Estimating value of Particle Matter in different algorithm model

Dates before and during MCO	**10 March 2020 (Before MCO)**		**26 March 2020 (During MCO)**	
No. Algorithm	**Min**	**Max**	**Min**	**Max**
Model 1	-89.41	-34.19	-88.30	-62.85
Model 2	-34.92	21.15	-40.55	-10.14

Model 3	60.03	131.58	52.86	91.66
Model 4	108.84	195.14	100.66	146.86
Model 5	24.12	92.57	17.30	55.21
Model 6	-84.08	-36.15	-88.74	-63.57
Model 7	25.57	83.51	19.58	50.52
Model 8	-60.24	-17.14	-64.22	-39.35

4.4 Pattern of PM10 phase before and during Movement Control Order (MCO) over Johor Bahru

After statistical findings, the developed regression model shows how well the spatial variation in air pollution can be predicted by applying the various regression models developed. In this section, we will analyze the water quality pattern affected by the COVID-19 effect. A map will be displayed to determine the pattern before and after the MCO. In this study, there are two different dates namely on 10 March and 26 March where we will identify changes in PM10 concentration in the study area. These changes can show whether the implementation of MCO can reduce pollution or vice versa.

4.4.1 PM_{10} concentration before and during Movement Control Order (MCO) lockdown phase over Johor Bahru

MCO was found to reduce PM10 concentration. Prior to the implementation of MCO and during MCO (10 March – 26 March 2020), daily PM10 concentrations were in the range of 47.9–136.77 μg/m3 and 25.82–110.50 μg / m3 respectively. The New Malaysia Ambient Air Quality Standard (NMAAQS) has set the standard PM10 limit to 100 μg / m3 for an average of 24 hours (Department of Environment Malaysia 2020)

and the World Health Organization (WHO) (2018) has set a stricter PM10 limit to 50 µg / m3. Table 4.3 shows PM10 concentration differences before and during MCO. Prior to the MCO, one of the air quality measurements from the satellite image exceeded the limit was model 4 (136.77µg / m 3), while during the MCO, the PM10 concentration exceeded limit by 110.50 µg / m 3. and during MCO. Based on the reading from table 4.3 the highest reduction is in model 1 with 138.09% (Before = -13.31 µg / m 3; During MOC = 18.38 µg / m 3), but in terms of measurement before MCO there is a disturbance, with value (- negetive) because based on the reading from the Department of Environment (DOE), the reading of particle of matters (PM10) has no value (- negative) as well as the reading from models 1,6 and 8. Logically, the actual reading of the highest reduction is in model 5 with 47.14% (Before = 48.85 µg / m 3; During MOC = 25.82 µg / m 3), while the lowest decreased was in model 4, with 19.20% (decrease at 23.03 µg / m 3). The proposed algorithm (algorithm model 5) was selected based on the highest decrease with -47.14% and the decrease value between before and after MCO with 23.02 µg / m 3. Figure 4.3 – 4.10 shows PM10 emission over Johor Pasir Gudang before (10 March 2020) and during (26 March) lockdown session in different measuring models.

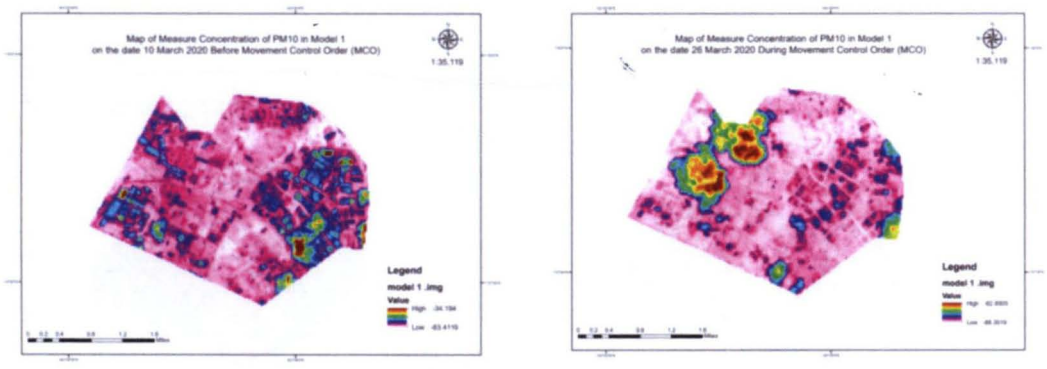

Figure 4.3 PM_{10} emission over Pasir Gudang before (10 March 2020) and during (26 March 2020) lockdown session in Model 1

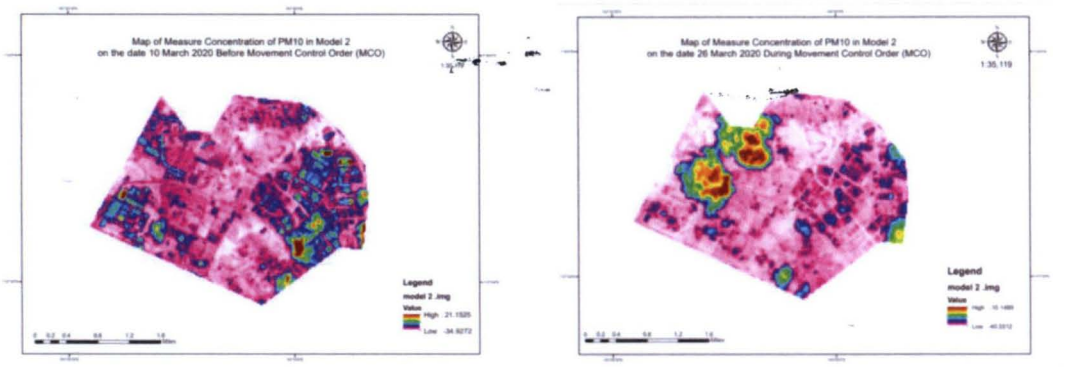

Figure 4.4 PM_{10} emission over Pasir Gudang before (10 March 2020) and during (26 March 2020) lockdown session in Model 2

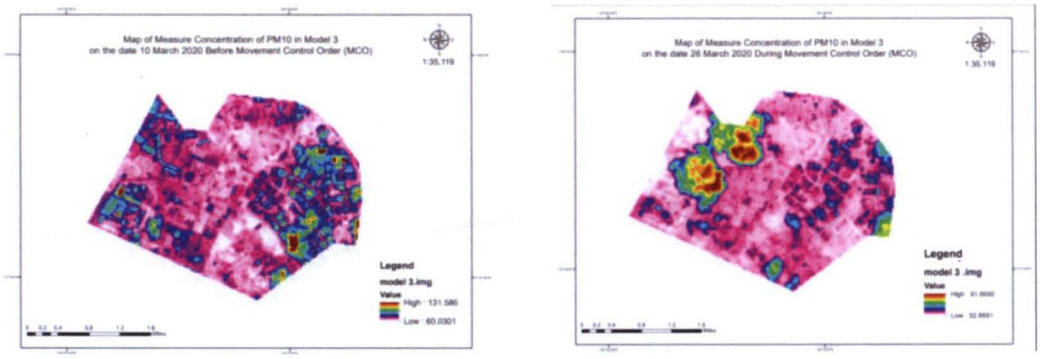

Figure 4.5 PM_{10} emission over Pasir Gudang before (10 March 2020) and during (26 March 2020) lockdown session in Model 3

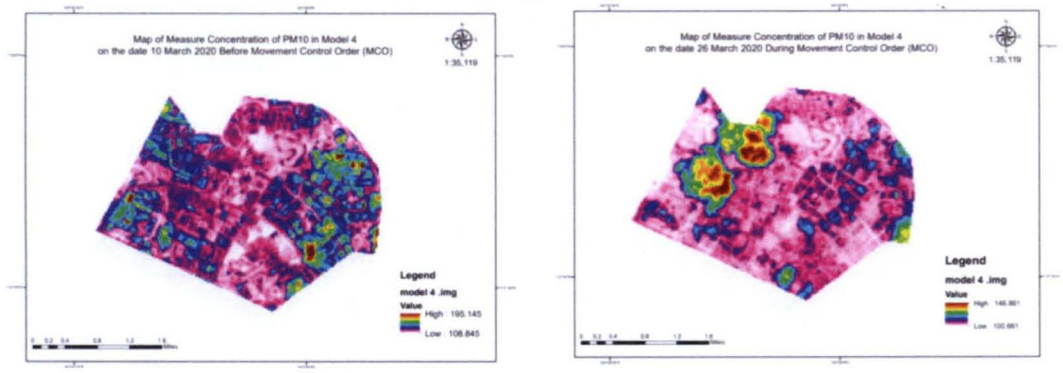

Figure 4.6 PM_{10} emission over Pasir Gudang before (10 March 2020) and during (26 March 2020) lockdown session in Model 4

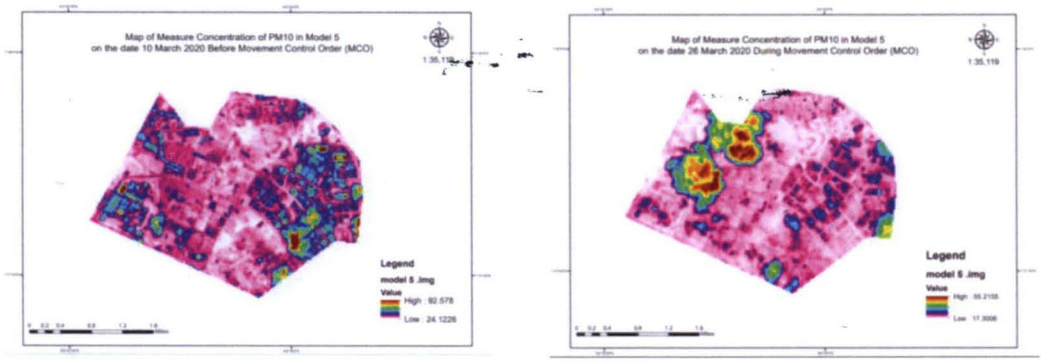

Figure 4.7 PM_{10} emission over Pasir Gudang before (10 March 2020) and during (26 March 2020) lockdown session in Model 5

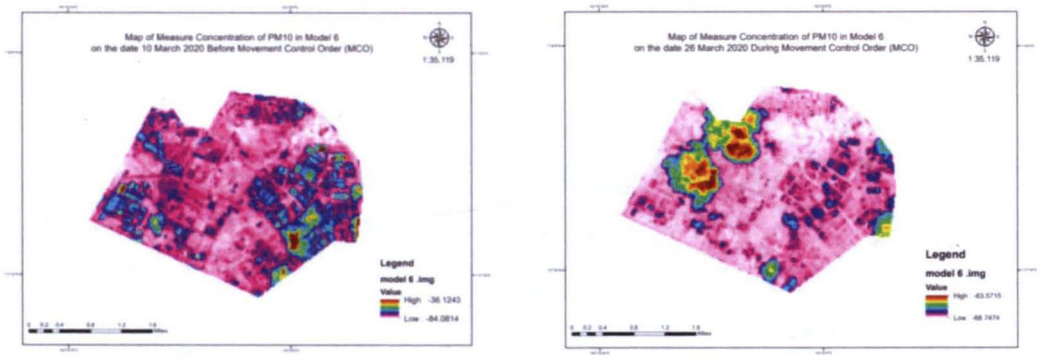

Figure 4.8 PM_{10} emission over Pasir Gudang before (10 March 2020) and during (26 March 2020) lockdown session in Model 6

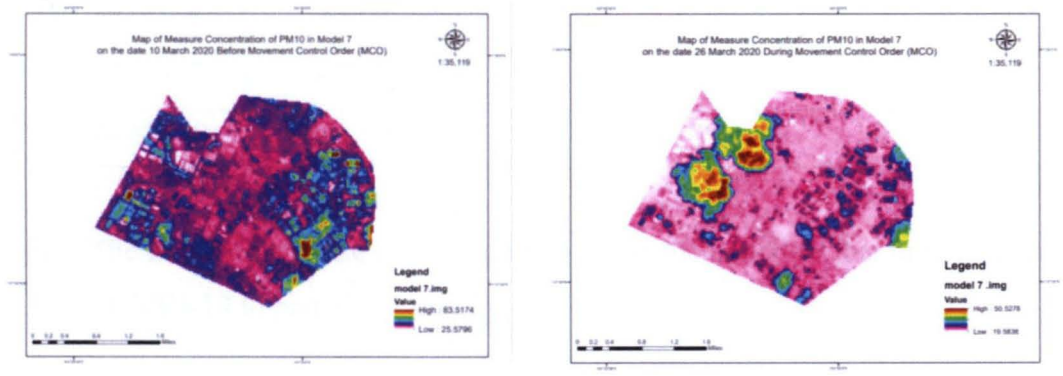

Figure 4.9 PM_{10} emission over Pasir Gudang before (10 March 2020) and during (26 March 2020) lockdown session in Model 7

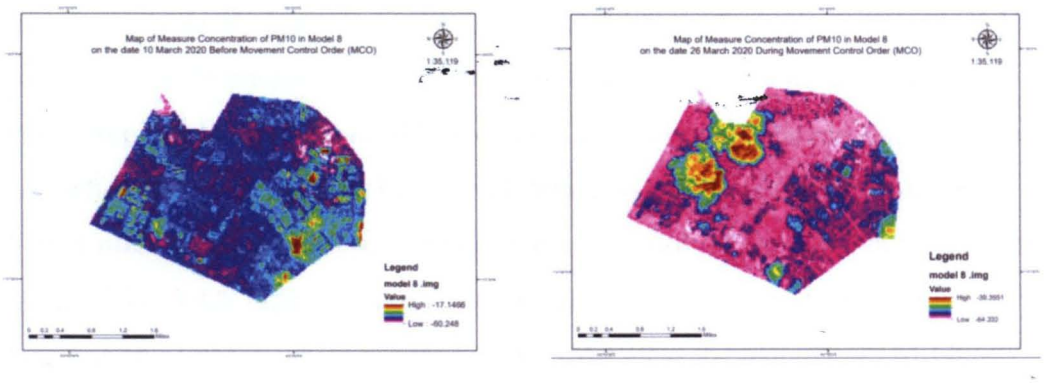

Figure 4.10 PM_{10} emission over Pasir Gudang before (10 March 2020) and during (26 March 2020) lockdown session in Model 8

Table 4.2 Variation of PM_{10} concentrations before MCO and during MCO

Model no.	Average of emission of PM_{10} before and during MCO			
	10 March 2020 before MCO	26 March 2020 during MCO	Variation	
			$\mu g/m^3$	Change (%)
Model 1	-63.21	-81.61	-18.4	+29.10
Model 2	-13.31	-31.69	-18.38	+138.09
Model 3	85.53	61.68	-23.85	-27.88
Model 4	136.77	110.50	-26.27	-19.20
Model 5	48.85	25.82	-23.03	-47.14
Model 6	-65.02	-82.39	-17.37	+26.71
Model 7	47.94	27.15	-20.79	-43.36
Model 8	-44.65	-58.92	-14.27	+31.95

4.4.2 The fluctuation of the concentration of particulate matters that impact from COVID-19 to pattern air quality

The MCO in Malaysia includes several restrictions on mass movement and assembly; Malaysians travel abroad; influx of tourists and visitors; and closure of educational institutions, government and private agencies. These restrictions can indirectly reduce air pollution in Malaysia, although detailed studies need to be done by considering other influential factors, including local meteorology and anthropogenic emissions.

There are several red zone areas in Johor Bahru with more than 41 confirmed COVID-19 cases (Crisis Preparedness and Response Center, 2020). Some red zone areas were later enforced under the Enhanced Movement Control Order. The red zone area covers Johor, where there are changes before and during the MCO as shown in figure 4.11 in different measurement models. Through the calculation of the various models used, only models 3,4,5 and 7 show the accuracy calculation in determining the concentration of PM10 where model 3 shows a decrease in change from 61.68 μg / m3 – 85.53 μg / m3 (-23.85 μg / m3), model 5 showed a decrease of -23.03 μg / m, model 7 showed a decrease of -20.79 μg / m3 while model 4 showed the most decrease with -26.27 μg / m3 with a combination of band 1 and band 2. Based on the results, implementation The MCO has successfully reduced the emissions of pollutants, especially the PM10 concentration, due to the lack of motor vehicles and current industrial activities of the MCO, this will change the pattern of air quality. In addition, the values in models 1,2,6, and 8 indicate values (-negative), this may involve images taken by satellites at the time including many clouds at the time or there may be interference taking pictures from there. From the DOE actual value reference, it shows the value before MCO with 31.94 μg / m3 and the value during MCO with 14.42 μg / m3. This indicates a very drastic decrease of 17.52 μg / m3 (54.85%) (DOE, 2020). As a result, the COVID-19 pandemic had a huge impact on most aspects areas of human activities, as well as on the economic and health systems. Closing, quarantine and border closure following the outbreak resulted in a decrease in air emissions due to decreased traffic and development. It's clearly, through observation the decrease in PM10 concentration mostly occurs after MCO announce. The movement and activities of residents living in red zone areas may have been restricted; However, pollution emissions, especially from mobile sources are indirectly reduced in the Johor Bahru area.

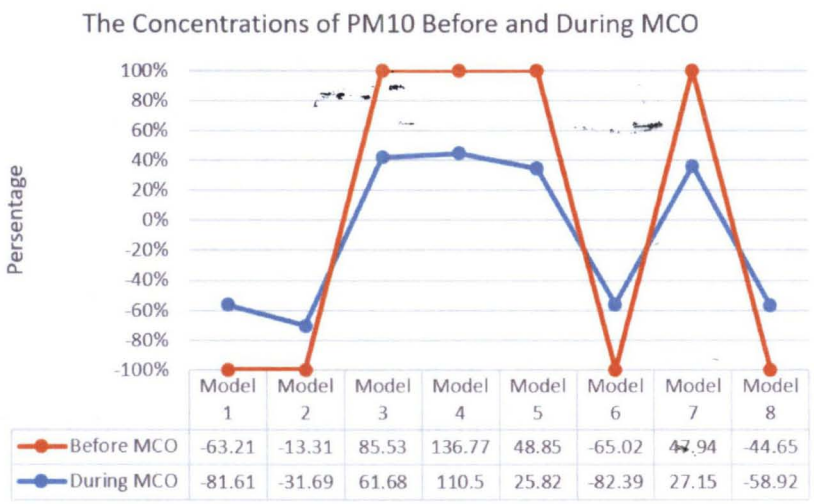

Figure 4.11 Reduction average based on different model

4.5 Map distribution of Particulate matter (PM_{10})

The usual mapping method, used to find out if the data follows a normal distribution, as happened in PM 10 which shows a slight slope as can be seen in Figure 4.12 – 4.15. The map is divided into 5 classes to estimate the spread of air pollution space in Pasir Gudang and the map also shows the color based on the reading determines the dominant air pollutant at the highest concentration where white color is considered lowest or very good, purple color is considered low or good, mint green color is considered moderate or light, mustard is considered high or unsafe, and maroon is considered very high or dangerous. These maps show that PM10 is mostly concentrated in the east, and west and especially in the central region of Johor, following major roads and urban nuclei, where PM10 even exceeds the annual average limit for human health protection set as 50 μ g / m 3. The distribution for PM 10 indicates that the most affected areas are areas in the southern and eastern provinces but without exceeding the set annual average limit. In the PM10 map, it can be seen how rural zones away from large agglomerations are more affected by these high levels of pollution (maroon and mustard).

Finally, the analysis was used to study the distribution of PM_{10} pollution levels in recent times after our country was hit by the spread of the COVID-19 epidemic. A

distribution map of PM_{10} for two dates namely 10 March 2020 and 26 March has been prepared for 4 different algorithm models. The trend of PM10 level decline has been observed in algorithms 3,4,5, and 7. This algorithm model was chosen, this is because the readings show the actual value according to DOE data.

The average diffusion of PM10 concentrations in Pasir Gudang, Johor Bahru before and after MCO is shown in Figure 4.12 – Figure 4.15. The average spread of PM10 concentration in dates 10 March 2020 before MCO and 26 March 2020 during MCO is in the range of 25 - 136 µg / m3. The higher average concentration of PM10 is around 100 - 180 µg / m3, it is shown in model 4 for the two dates in figure 4.13. PM10 of mean concentration on 10 March 2020 with 80 -100 µg / m3 while mean concentration on 25 March 2020 with 60 – 80 µg / m3. In model 5 shows a lower PM10 concentration between 15 - 75 µg / m3 where the highest mean concentration of PM10 on 10 March 2020 with 45 – 60 µg / m3 while the highest mean concentration on 25 March 2020 with 30 – 45 µg / m3. Next, model 3 shows about 40 - 120 µg / m3 PM10 concentration. Model 7 shows about 15 - 80 µg / m3 PM10 concentration.

Using the average air pollution and meteorological data on, the figures show that all air pollutants except in models 1,2,6 and 8 show a similar decline trend during the MCO from the same period in 2019. Based on DOE data, shows a decrease between 14 - 39 µg / m3. This proves that air pollution before and during MCO shows significant changes and shows an advantage in a good environment. The decline can be identified from the unexpected consequences of the economic closure almost stalled as the COVID-19 outbreak gave clear skies in places notorious for poor air quality. According to (Abdullah et al., 2020) , on April 30, 2020, there has been a 26% increase in the good Air Pollution Index (API) days throughout Malaysia since the MCO began. MCO not only reduces the spread of COVID-19 among community members but also reduces environmental pollution due to reduced anthropogenic activity.

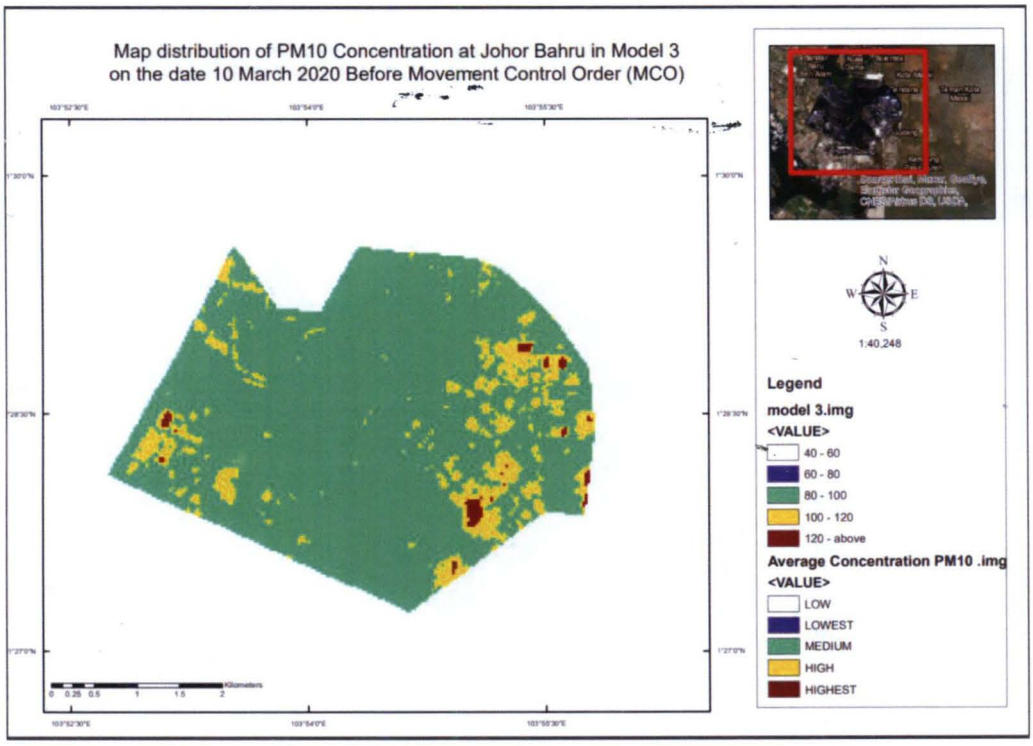

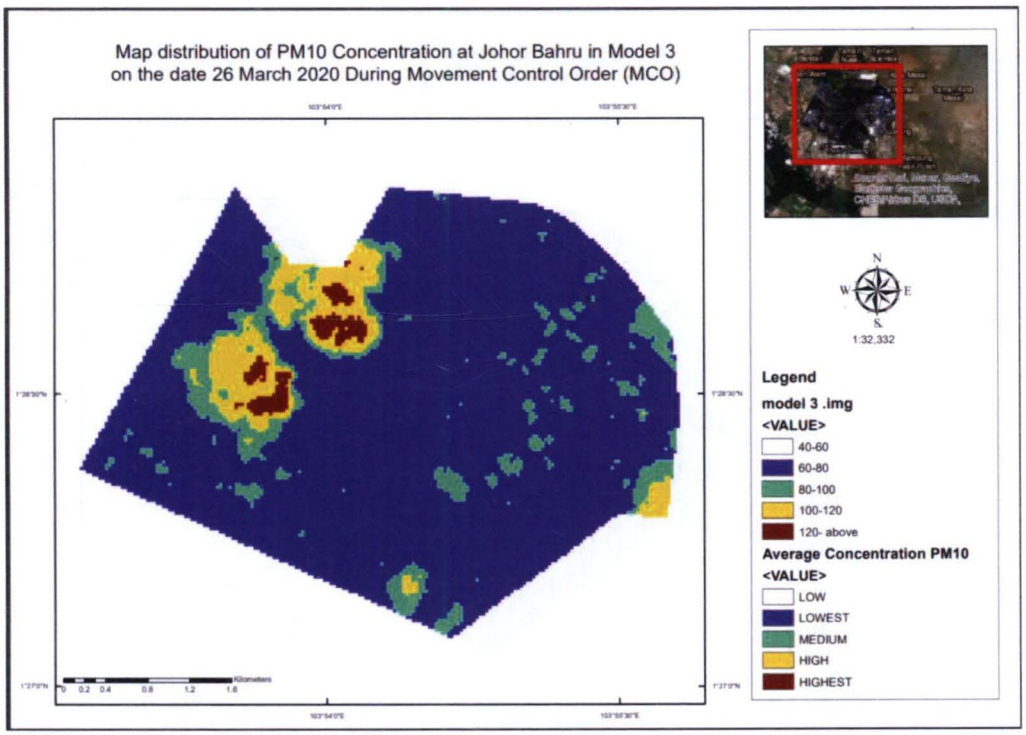

Figure 4.12 Map distribution of PM_{10} Concentration at Johor Bahru before and during MCO in model 3

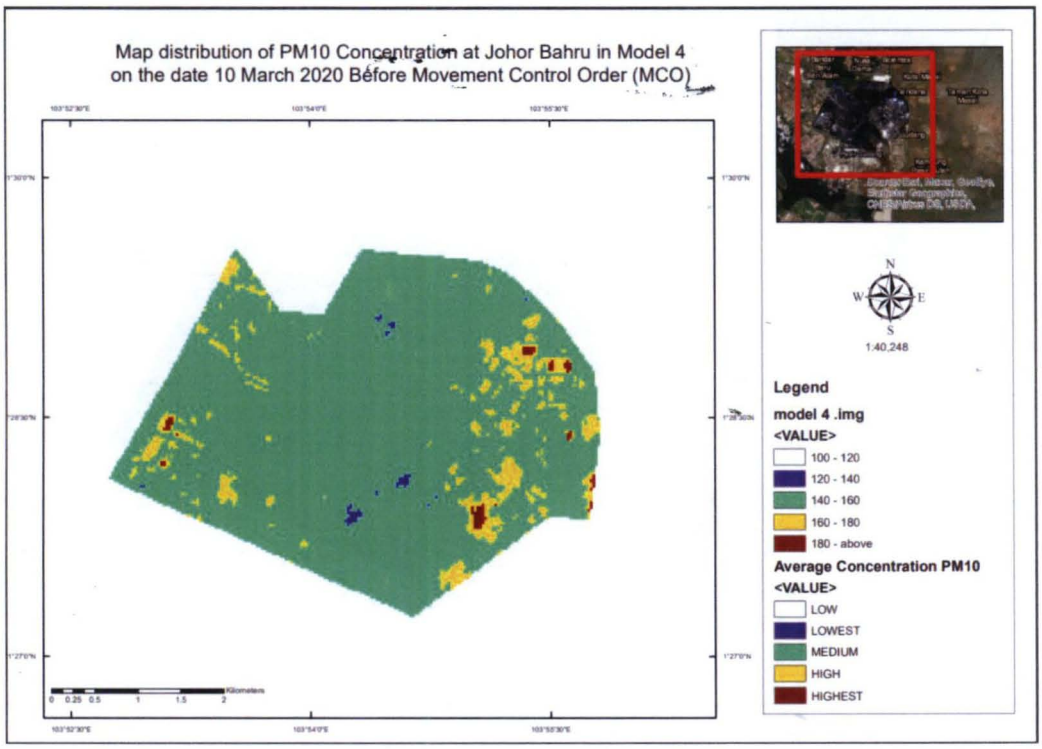

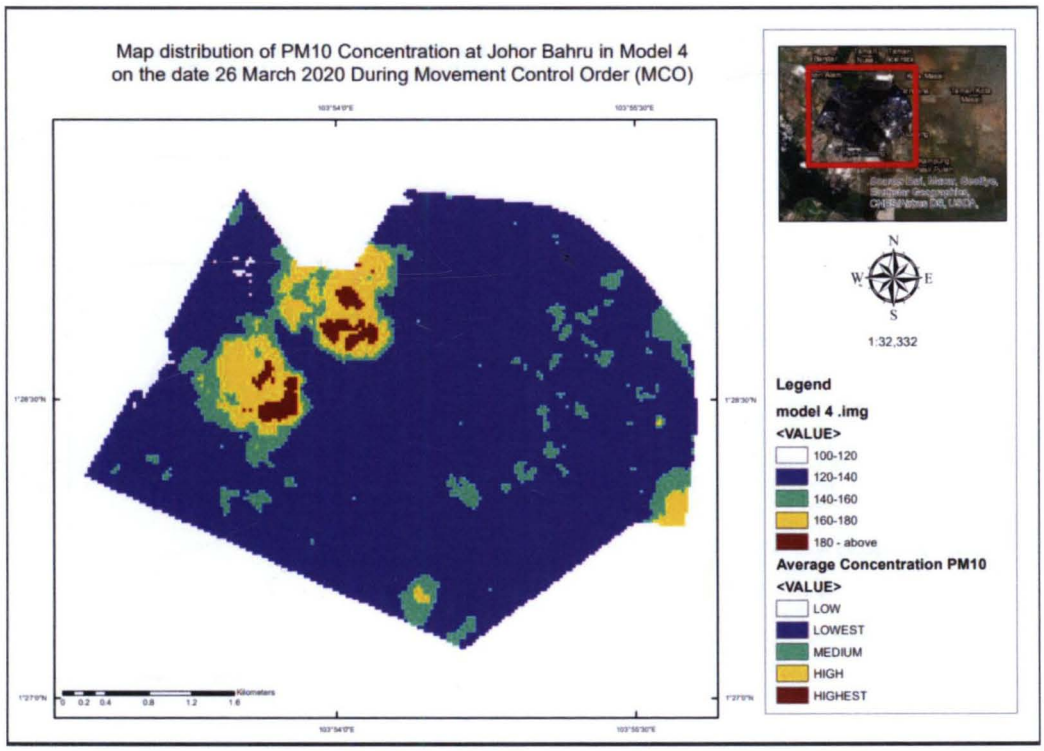

Figure 4.13 Map distribution of PM_{10} Concentration at Johor Bahru before and during MCO in model 4

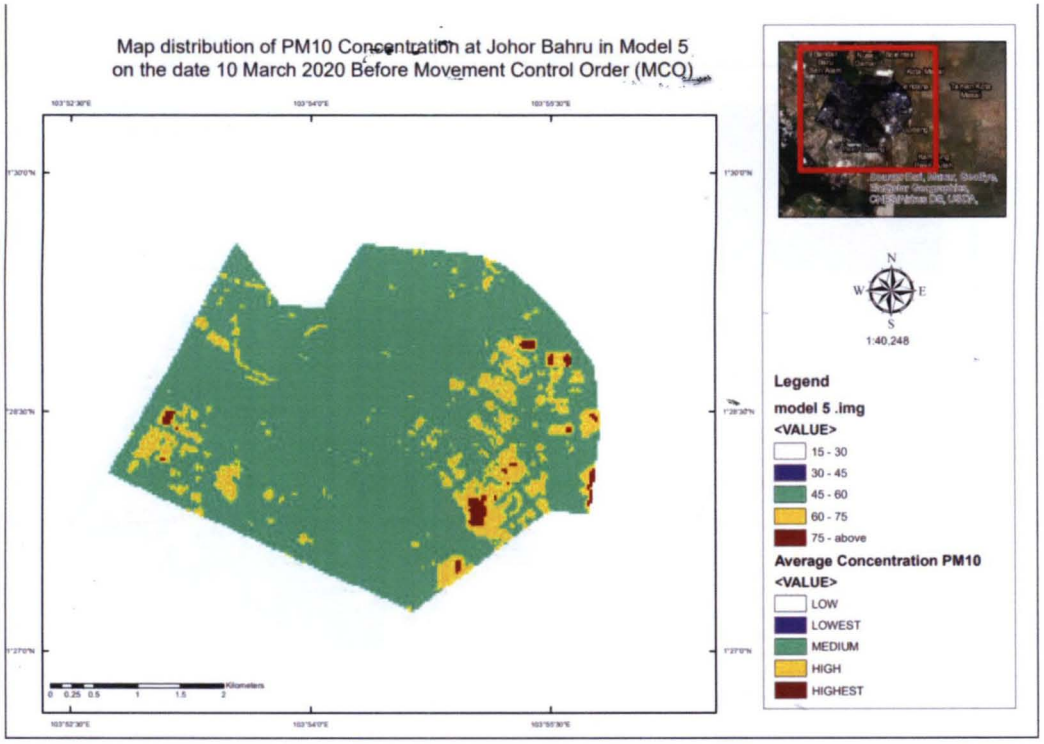

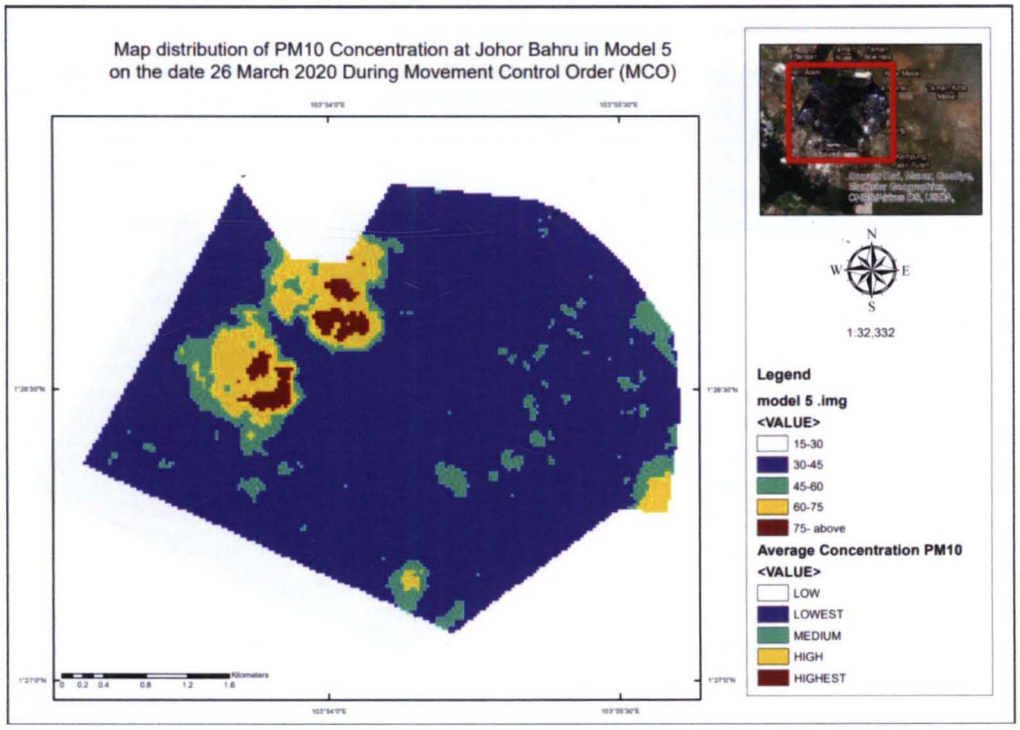

Figure 4.14 Map distribution of PM_{10} Concentration at Johor Bahru before and during MCO in model 5

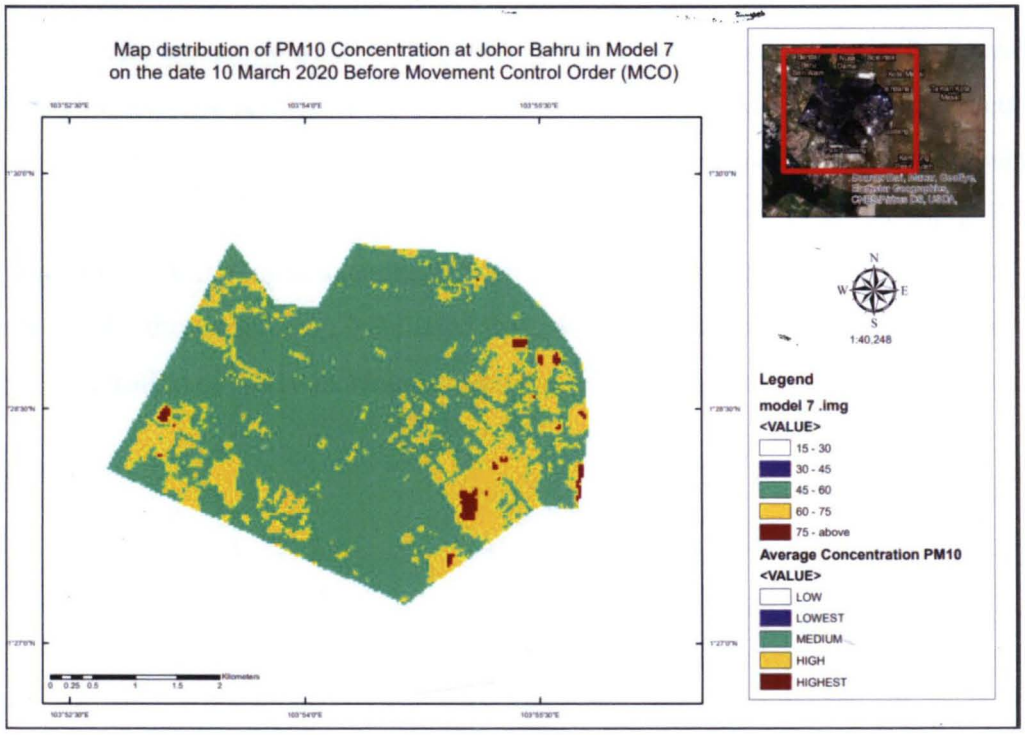

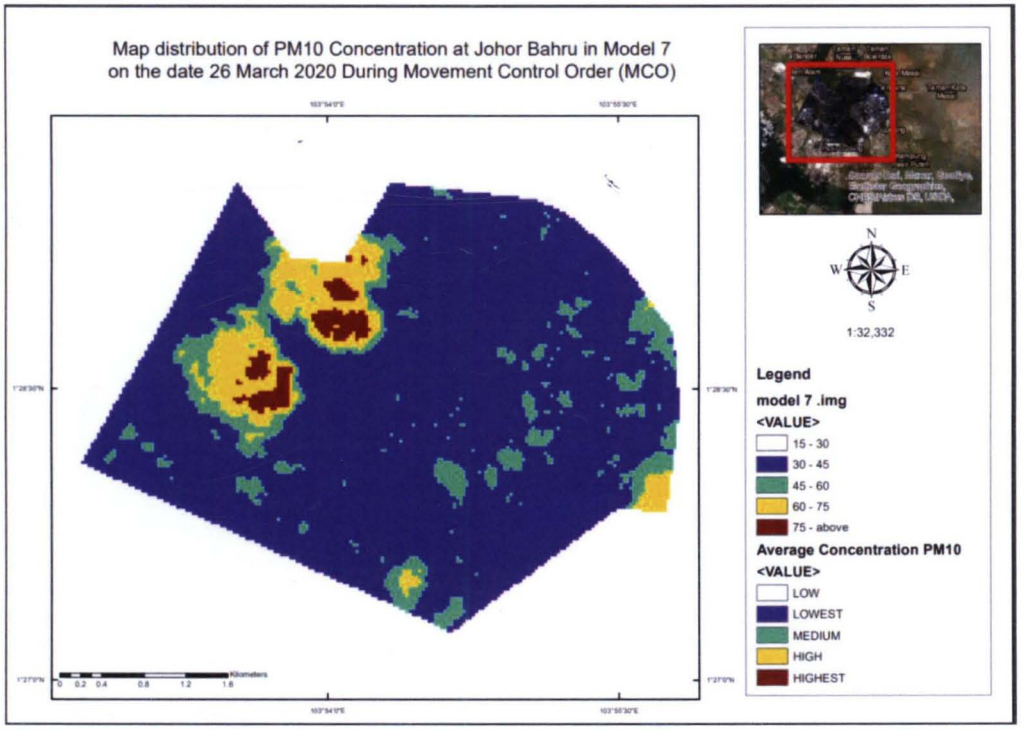

Figure 4.15 Map distribution of PM_{10} Concentration at Johor Bahru before and during MCO in model 7

4.6 Summary of Chapter

All the results and analyzes that have been identified have been extensively discussed in this chapter. The results of the proposed multispectral PM10 model can calculate the concentration of PM10 using atmospheric reflection on the Landsat 8 band which can be seen with a high degree of accuracy. This adds to evidence of a linear relationship between particle concentration and atmospheric reflection visible stripes. In this study, the researchers concluded that MCO has a significant effect in reducing the concentration of PM10 in Malaysia and there is a change in the pattern of air quality

CHAPTER 5

CONCLUSION AND RECOMMENDATION

5.1 Introduction

This chapter described about all the studies that have been carried out and the analyses of the results. The study consists of three stages; i) data selection and study area, ii) data processing, and iii) data analyses. Data have been used in this study are air quality data for PM10 which is derived from satellite image and carried out the calculation measure concentration of PM10 by different algorithm model from citation (Saraswat et al., 2017)

5.2 Conclusion

Below is the summary of the finding of this study. It will discuss all about the final result of this study.

5.2.1 Measurement of Particulate Matter

The first objective is to measure the PM10 concentrations using a spatial modeler from ERDAS IMAGINE software of both dates on 10 March 2020 and 26 March 2020 located in Johor Bahru. The algorithm used from the quotation (Saraswat et al., 2017) produces a high correlation between the measured and calculated PM10 concentrations. The study proved the efficiency of their multispectrum estimation model with PM10 concentration based on Landsat 8 OLI band which can be seen in satellite images with Johor region.

5.2.2 Pattern of Air Quality

The second objective is to determine the impact of COVID-19 on the pattern of air quality on both dates before and during MCO. The mean values during MCO and

before MCO are required to see the difference and the calculation actual reading of the highest or reduction in that shown $\mu g / m 3$ or percent. The result has generated the implementation of MCO successfully reduced the emissions of pollutants, especially PM10 concentration, due to lack of motor vehicles and industrial activities during MCO, this will change the pattern of air quality.

5.2.3 Regression Analysis

The final objective of this research is to map the distribution of air pollutants for the research area. A distribution map of PM10 for two dates namely 10 March 2020 and 26 March has been prepared for 4 different algorithm models. Regression analysis was carried out after making measurements concentration PM10 using the spatial modeler, then its shows the pattern of air quality on dates 10 March 2020 before MCO and 26 March 2020 during MCO. Each algorithm shows different results in rates minimum and maximum in the study area. In observations, it can be shown that PM10 is mostly concentrated in the east, west, south, and especially in the central region of Johor, following the main roads and the core of the city.

5.3 Recommendation

If there are any attempts to continue this research in future, several recommendations should be taken into consideration as follows.

1) In order to achieve a relationship between atmospheric correction recommendation in this study, application the atmospheric FLAASH correction in ENVI software or ATCOR atmospheric correction is in ERDAS image software. FLAASH and ATCOR atmospheric correction were applied simultaneously and given better results for FLAASH atmospheric correction for images
2) In this study, only focus on one monitoring station, namely Pasir Gudang. To be more interesting, also select other monitoring stations to study each station differently. Moreover, if we selected more than 5 stations we can add the station on map and create interpolation map.

3) Study the air pollution concentration with relation to determine between ambient air pollution and meteorological parameters such as air temperature.

4) Study to explore the difference of LST of the city before and after total lockdown.

BIBLIOGRAPHY

Abdul Hamid, H., Hanafi Rahmat, M., & Aisyah Sapani, S. (2018). The classification of PM10 concentrations in Johor Based on Seasonal Monsoons. *IOP Conference Series: Earth and Environmental Science*, *140*(1). https://doi.org/10.1088/1755-1315/140/1/012028

Abdullah, S., Mansor, A. A., Napi, N. N. L. M., Mansor, W. N. W., Ahmed, A. N., Ismail, M., & Ramly, Z. T. A. (2020). Air quality status during 2020 Malaysia Movement Control Order (MCO) due to 2019 novel coronavirus (2019-nCoV) pandemic. *Science of the Total Environment*, *729*(January). https://doi.org/10.1016/j.scitotenv.2020.139022

Ahmad, K., Abdulla, A., & Koas, A. (2010). *GIS-based Mapping and Statistical Analysis of Air Pollution and Mortality in Brisbane, Australia*. *April*, 67.

APIMS. (2018). APIMS Air Pollutant Index of Malaysia. *Air Pollutant Index of Malaysia Announcement*, 2018.

ASMA. (2015). Manual Air Quality Monitoring (MAQM). *Alam Sekitar Malaysia Sdn. Bhd.*, 3–6. https://www.doe.gov.my/portalv1/wp-content/uploads/2013/01/Air-Qulaity.pdf

Basly, Ludovic, and Baleynaud, J.-M. S. (2020). *ata for the air pollution mapping Basly détection & Modélisation , Centre d ' Energétique , Ecole des Mines de Paris , France universitaire de Calcul de Toulouse , France*. *2020*, 1–15.

Briggs, D. J., Collins, S., Elliott, P., Fischer, P., Kingham, S., Lebret, E., Pryl, K., Van Reeuwijk, H., Smallbone, K., & Van Der Veen, A. (2010). Mapping urban air pollution using gis: A regression-based approach. *International Journal of Geographical Information Science*, *11*(7), 699–718. https://doi.org/10.1080/136588197242158

Buseck, P. R.; Schwartz, S. E., & It. (2021). *NASA / ADS*. 2–5.

Chee Khoon, C. (2008). Haze causes not just discomfort , it kills. *Malaysia Kini, February 2002*, 4–6. http://www.malaysiakini.com/letters/57929

Chooi, Y. H., & Yong, E. L. (2016). The Influence of PM 2 . 5 and PM 10 on Air Pollution Index (API). *Faculty of Civil Engineering, Universiti Teknologi Malaysia, Malaysia*, 132–143.

DOE. (1997). A Guide to Air Pollutant Index in Malaysia. In *Department of Environment* (Vol. 3rd, p. 6).

DOE. (2013). New Malaysia Ambient Air Quality Standard. *Department of Environment , Malaysia*, 1989. http://www.doe.gov.my/portalv1/wp-content/uploads/2013/01/Air-Quality-Standard-BI.pdf

DOE. (2020). *Official Portal of Department of Environment Enforcement The Compliance Of EQ (Scheduled Waste) Regulation 2005 Through System eSWIS*. 1–2.

Dr. I.C. Agrawal, Dr. R.D. Gupta, E. V. K. G. (2003). Map India 2003 Environment Pla GIS as modelling and decision support tool for air quality management : a conceptual framework. *Environment Planning, Map India Conference 2003*, 1–12.

EPA, U. E. P. in N. E. | U. (2005). What is particulate matter? *Particulate Matter in the United Kingdom*, 16–28. https://uk-air.defra.gov.uk/assets/documents/reports/aqeg/ch2.pdf

Gardiner, B. (2020). Pollution made COVID-19 worse. Now lockdowns are clearing the air. *Science: Coronavirus Coverage*, 3–7. https://www.nationalgeographic.com/science/2020/04/pollution-made-the-pandemic-worse-but-lockdowns-clean-the-sky/

Gupta, E. V. K. D. I. C. A. R. D. G. (2009). Remote Sensing and GIS as an Information Technology for Air Quality Status Planning. *Geospatial World* -, 3–5.

Hanafi, N. H., Hassim, M. H., & Noor, Z. Z. (2018). Overview of health impacts due to haze pollution in Johor, Malaysia. *Journal of Engineering and Technological Sciences*, *50*(6), 818–831. https://doi.org/10.5614/j.eng.technol.sci.2018.50.6.5

Hasfazilah Ahmat*, A. S. Y. & N. A. R. (2019). People on love drug MDMA still know w. *Sains Malaysian*, *2019*(21), 1–16.

Iwona S. Stachlewska, Olga Zawadzka, R. E. (2007). Introduction : Methodology : Results : *MDPI*, *15*(2005), 2007.

Khairuddin, D. L. (2020). Nitrogen dioxide levels decrease due to MCO. *Covid-19 | Think City Analytics Team*, 3–8.

Lim, H.-S., Mat Jafri, M. Z., & Abdullah, K. (2010). Algorithm For Air Quality Mapping Using Satellite Images. *Air Quality*, *2020*, 1–17. https://doi.org/10.5772/9762

Love, M. C. (2020). Air Pollution, COVID-19 and Earth Day - Scientific American Blog Network. *Scientific American Blog Network*, 1–13. https://blogs.scientificamerican.com/observations/air-pollution-covid-19-and-earth-day/

MEER, F. D. VAN DER. (1991). A comparison of conventional classification methods and a new indicator kriging based method using high-spectral resolution images (a viris) freek d. van der meer. *International Institute for Aerospace Survey and Earth Sciences (ITC) Department of Earth Resources Surveys Research Scientist in Geological Survey*, 72–79.

Mohd Zamri Ibrahim, M. I. and Y. K. H. (2016). We are IntechOpen , the world ' s leading publisher of Open Access books Built by scientists , for scientists TOP 1 %. *Intech*, *i*(tourism), 13. https://doi.org/http://dx.doi.org/10.5772/57353

Nur H. Hanafi, M. H. H. Z. Z. N. D. K. S. N. N. H. N. 1, 1,*, 2, 3, & Helmi1, N. M. A. 1D. (2019). s of transported pollution and haze-related diseases via HYSP ory Modelling in the urbanized area of Johor , Malaysia. *Conf. Series: Earth and Environmental Science*, *2020*, 1–13.

Nurol. (2015). *Melahu Enjin Kenderaan Ancaman Kesihatan dan Persekitaran Amaran Don*. 4–9. https://news.utm.my/ms/2015/04/melahu-enjin-kenderaan-ancaman-kesihatan-dan-persekitaran-amaran-don/

Projek, T., & Tepat, H. S. R. (2021). *Hikmah PKP : Bila alam berbicara melalui kualiti*. 1–5.

Samanta, S., Pal, B., & Pal, D. K. (2011). *Modeling of Monthly Mean Air Temperature through Remote Sensing and GIS techniques*. *3*(1), 85–92.

Saraswat, I., Mishra, R. K., & Kumar, A. (2017). Estimation of PM10 concentration from Landsat 8 OLI satellite imagery over Delhi, India. *Remote Sensing Applications: Society and Environment*, *8*(October), 251–257. https://doi.org/10.1016/j.rsase.2017.10.006

Savira, F., & Suharsono, Y. (2013). KESAN PEMBANGUNAN KAWASAN PERINDUSTRIAN TERHADAP KOMUNITI PESISIR PANTAI DI PASIR GUDANG, JOHOR. *Journal of Chemical Information and Modeling*, *01*(01), 1689–1699.

Shaheen, A., Kidwai, A. A., Ain, N. U., Aldabash, M., & Zeeshan, A. (2017). Estimating Air Particulate Matter 10 Using Landsat Multi-Temporal Data and Analyzing its Annual Temporal Pattern over Gaza Strip, Palestine. *Journal of Asian Scientific Research*, *7*(2), 22–37. https://doi.org/10.18488/journal.2/2017.7.2/2.2.22.37

Sharma, N., Bhandari, K., Rao, P., Scientists, A. S., Road, M., & Delhi, N. (2015). *GIS applications in air pollution modeling*. 1–9.

Sifakis, N., & Deschamps, P. Y. (1992). Mapping of air pollution using SPOT satellite data. *Photogrammetric Engineering & Remote Sensing*, *58*(10), 1433–1437.

Straits, T. H. E. (2021). *THE STRAITS 3 factories in Johor ' s Pasir Gudang found with high traces of toxic gases*. 1–7.

Thongplang, J. (2020). Particulate Matter : Why monitor. *(Https://Www.Aeroqual.Com/2020/04/06)*, 1–8.

Tiwari, S., Chate, D. M., Srivastava, A. K., Bisht, D. S., & Padmanabhamurty, B. (2012). *in Delhi at different mean cycles*. *29*.

USGS. (2012). What is Propan-2-ol and what is it used for ? *USGS Science for a Changing World*, 1–6. https://mistralhowto.wordpress.com/2012/03/07/what-is-propan-2-ol-bp-and-what-is-it-used-for/

Veefkind, P., van Oss, R. F., Eskes, H., Borowiak, a, Dentner, F., & Wilson, J. (2007). The Applicability of Remote Sensing in the Field of Air Pollution. *Framework*, 1–54.

WHO. (2018). 9 Out of 10 People Worldwide Breathe Polluted Air, But More Countries Are Taking Action. *Saudi Medical Journal*, *39*(6), 641–643.

Wikipedia. (2020a). 2020 coronavirus pandemic in Indonesia. *Wikipedia*, *2019*(January), 1–48. https://en.wikipedia.org/wiki/2020_coronavirus_pandemic_in_Indonesia

Wikipedia. (2020b). *Sources of atmospheric particulate matter Composition Size distribution of particulates*. 1–26.

APPENDICES

A. Steps for Layer Stack

a) Open ERDAS IMAGINE 2013 and the figure will appear

Figure 3.1A Erdas Imagine 2013 Icon Panel

b) Open the Raster tab on the menu selection, select the Spectal and open the Layer Stack tool

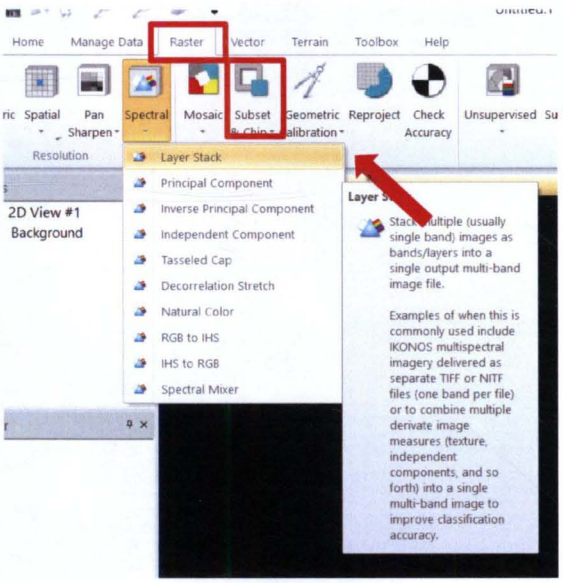

Figure 3.2A Set the Layer Stack

c) On the Layer Stack tool select the input files (Individual TIFF images Landsat Data) which select the band one image and ADD it to the layer list (corresponds

to the actual band number of the file from band 1-band 11). Once all bands have been selected added, specify the output file as layers for new image

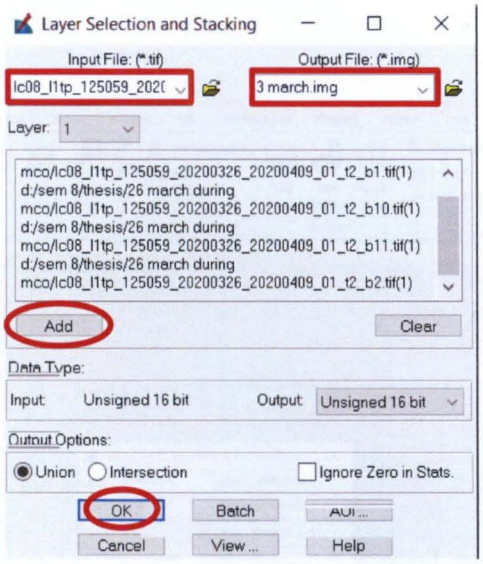

Figure 3.3A Window for add the layer band into one image

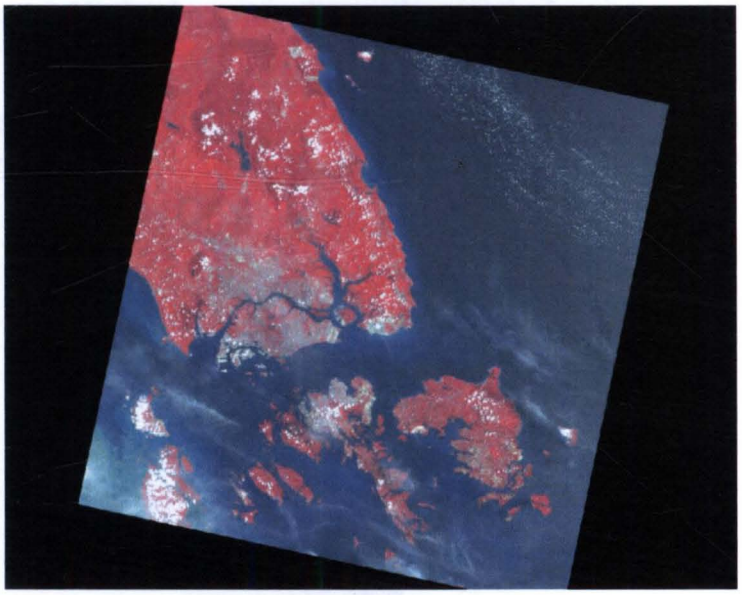

Figure 3.4A The result of layer stack in multi-band 5,4,3

B. Creating Subset Image

1) To subset the study area, go to inquiry options on the menu tab then select inquiry box. Resize the box according to the study area and click apply

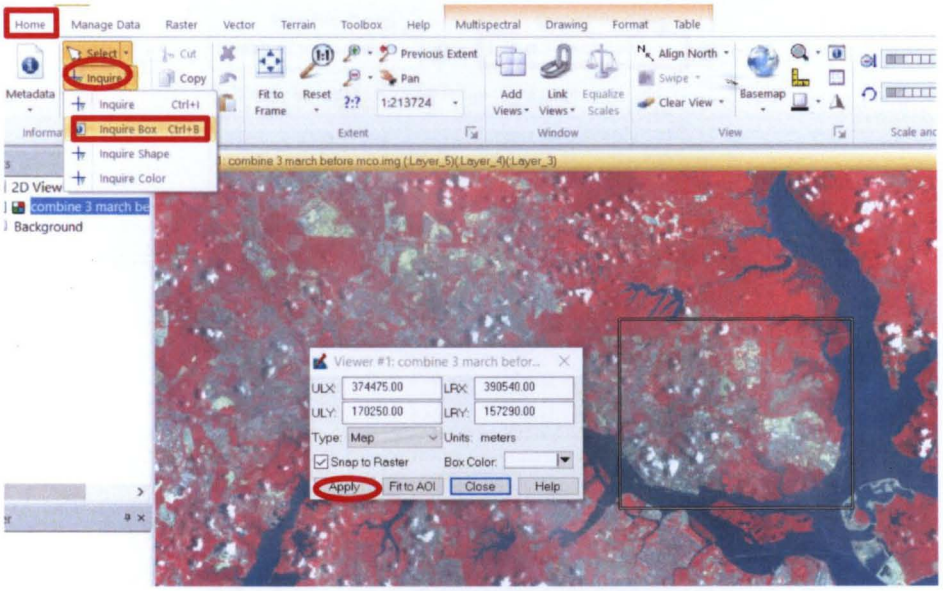

Figure 3.1B Set the inquiry box and resize the box into study area

2) go to the Raster tab and select Subset & Chip dropdown in the resolution tool and open the Create Subset Image.

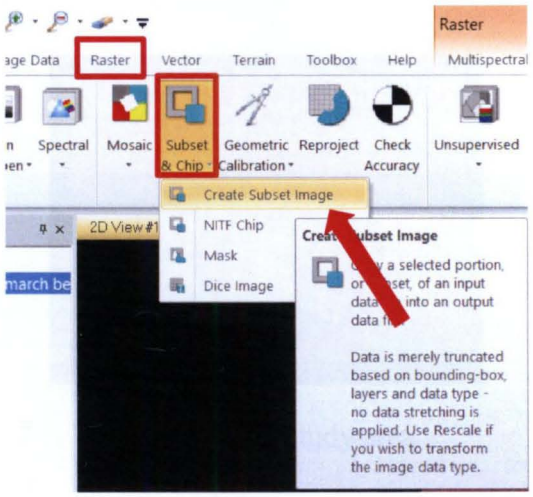

Figure 3.2B Create Subset window

3) On the subset tool, specify the output file as new subset file. Then click from Inquiry Box according the inquiry box that has been made as subset area and click OK. The result is shown in figure 3.4B

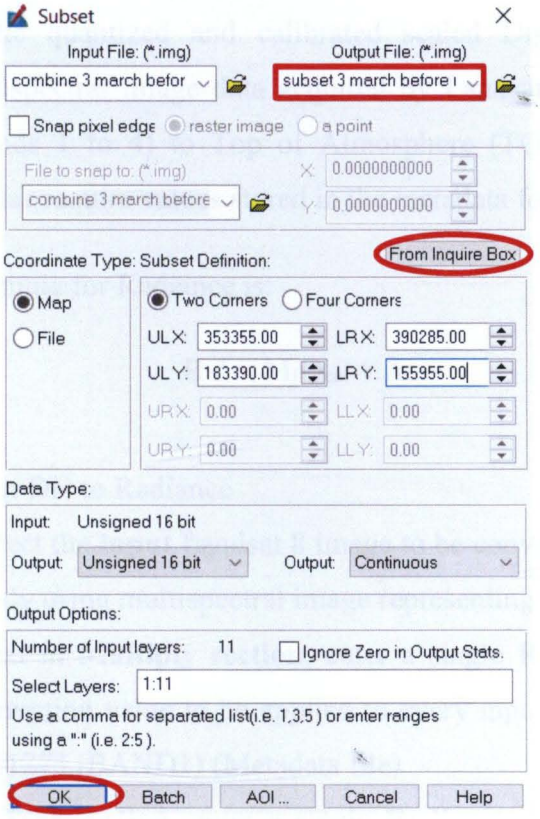

Figure 3.3B Window for Subset

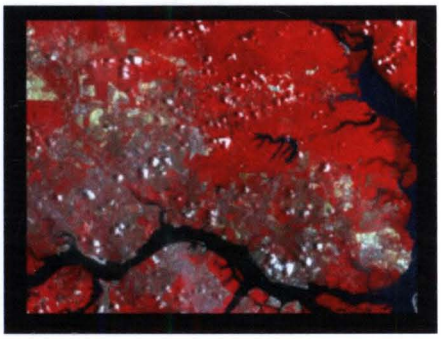

Figure 3.4B Study area

C. Landsat 8 Top of Atmosphere Reflectance Conversion

Spatial Modeler provides the user with hundreds of functions, algorithms and analytical routines that can easily be chained together into models that solve Geospatial problems. This model implements the formulas published by the USGS for converting the quantized and calibrated scaled Digital Numbers (DN) representing multispectral image data acquired by Landsat 8 Operational Land Imager (OLI, bands 1 to 4) to Top of Atmosphere (TOA) Reflectance. The conversion formulas require values stored in the metadata for each image;

The published formula for Radiance is:

$$R_I' = M_I Q_{cal} + A_L$$

i) Convert DN to Radiance

- Select the **input** Landsat 8 image to be convert to radiance, in this study using multispectral image representing bands 1 to 4 only.
- Next in **Multiply section**, enter a single **Radiance_Mult_Band** correction value to be applied to every input band. The default is 0.01273 (BAND1) (Metadata file)
- In **Plus section**, enter a single **Radiance_Add_Band** correction value to be applied to every input band. The default is -63.65072(Metadata file)
- Lastly, name the **output** image file containing the radiance values. This will be a 32-bit Float data type.

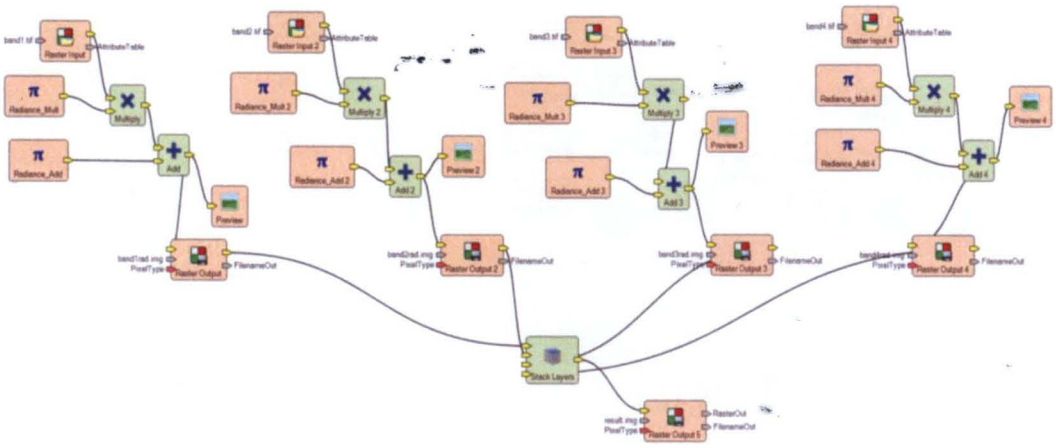

Figure 3.1C Convert DN to Radiance using Spatial modeler

The published formula for TOA Reflectance is:

$$R_{\lambda}' = M_{\lambda} Q_{cal} + A_r$$

ii) Convert Radiance to TOA Reflectance

- Select the **input** Landsat 8 image to be convert to TOA Reflectance, using image from radiance multispectral image
- Next in **Multiply section**, enter a single **Reflectance_Mult_Band** correction value to be applied to every input band. The default is 0.00002 (Metadata file)
- In **Plus section**, enter a single **Reflectance_Add_Band** correction value to be applied to every input band. The default is -0.1 (Metadata file)
- In **Divided section**, here used **SIN equation** then enter a single value for the **Sun's elevation** (in degrees) above the horizon at the time of image acquisition.
- Lastly, name the **output** image file containing the radiance values. This will be a 32-bit Float data type.

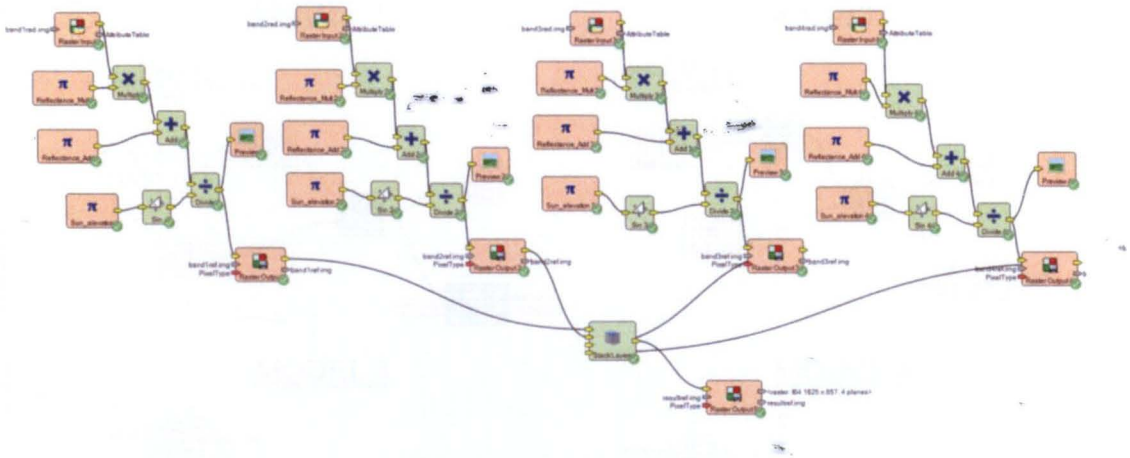

Figure 3.2C Convert Radiance to Reflectance using Spatial modeler

D. Calculation on measuring of concentration PM_{10}

The atmospheric reflectance was then related to the PM_{10} using the regression algorithm analysis, from there build calculate models PM_{10} as shown in Table 1, where we using spatial modeler to calculated the particulate matter concentration.

Model. No	Mathematical model
1.	$PM_{10} = R_{Band1}(24.45) - 83.4119$
2.	$PM_{10} = R_{Band2}(28.12) - 34.9272$
3.	$PM_{10} = R_{Band3}(35.81) + 60.0301$
4.	$PM_{10} = R_{Band4}(40.92) + 108.845$
5.	$PM_{10} = R_{Band1}(-25.78) + R_{Band2}(59.89) + 24.1226$
6.	$PM_{10} = R_{Band2}(43.45) + R_{Band3}(-20.12) - 84.0814$
7.	$PM_{10} = R_{Band3}(64.39) + R_{Band4}(-34.41) + 25.5796$
8.	$PM_{10} = R_{Band1}(-53.69) + R_{Band2}(134.26) + R_{Band3}(-60.70) - 60.248$

Figure 3.1D Algorithm model in different model

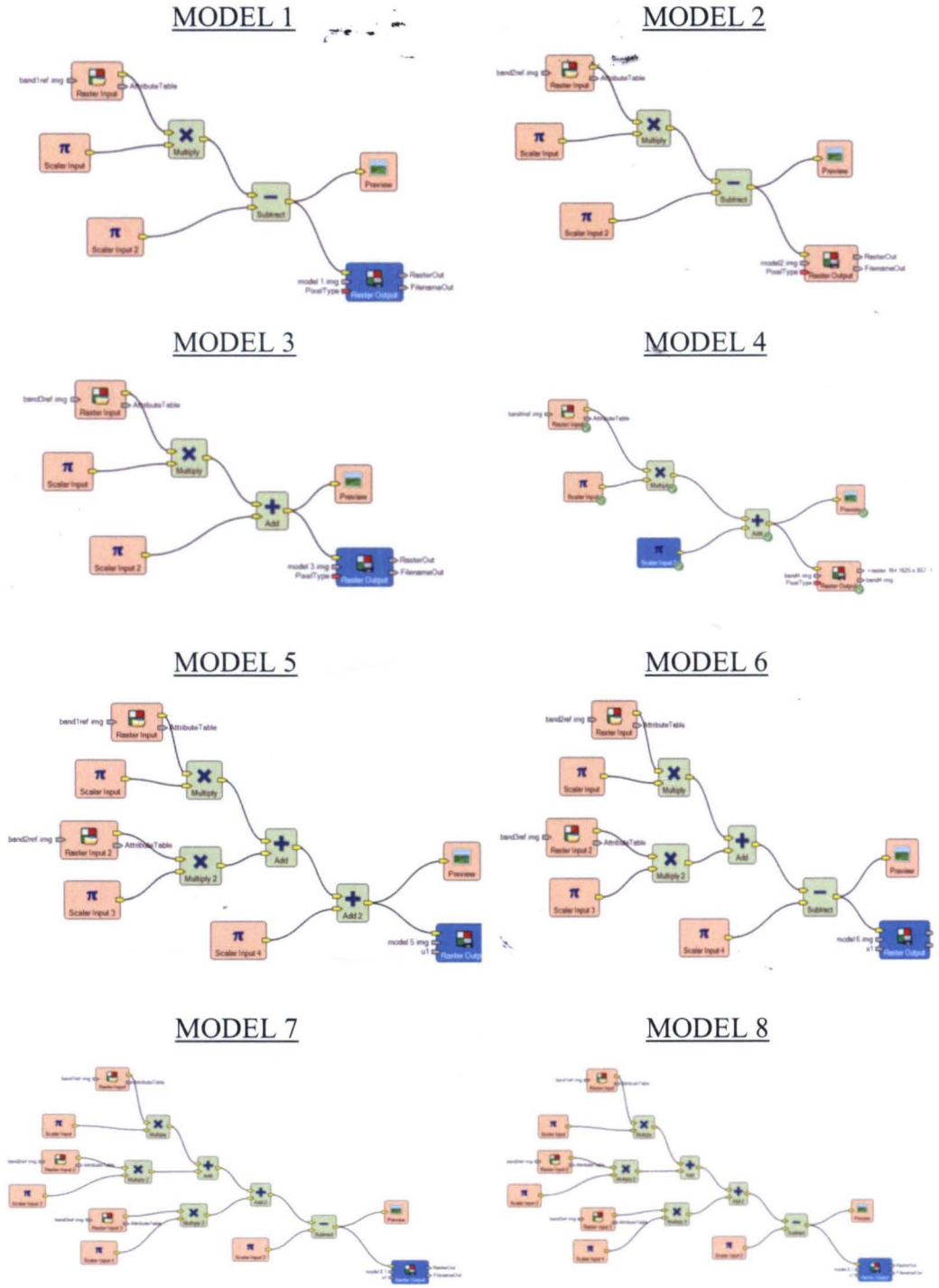

Figure 3.2D Spatial modeler using different types of algorithms for atmospheric reflectance in Band 1 (b1), Band 2 (b2), Band 3 (b3) and Band 4 (b4) of Landsat 8 images and ground measured PM_{10} values.